Nanoscale

Accepted Manuscript

This article can be cited before page numbers have been issued, to do this please use: E. Secor, D. Yeboah and L. Gamba, *Nanoscale*, 2025, DOI: 10.1039/D5NR02110C.

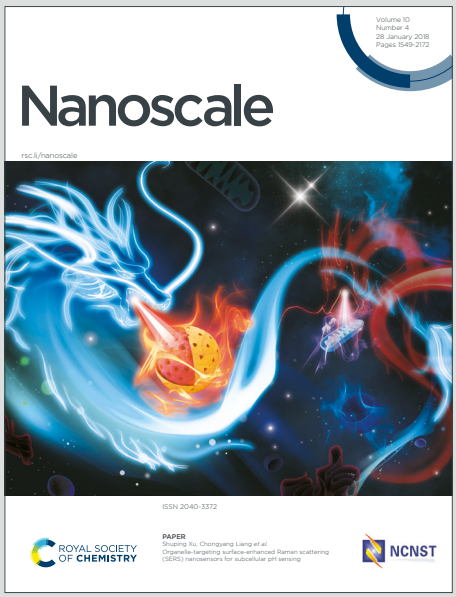

ROYAL SOCIETY OF CHEMISTRY

rsc.li/nanoscale

View Article Online
DOI: 10.1039/D5NR02110C

REVIEW

Additive electronics manufacturing via droplet jetting technologies: Materials, methods, applications, and opportunities

Ethan B. Secor,* Daniel Yeboah, and Livio Gamba

Received 00th January 20xx,
Accepted 00th January 20xx

DOI: 10.1039/x0xx00000x

Droplet jetting technologies offer a versatile, digital platform to fabricate functional devices from nanomaterial building blocks. Inkjet, aerosol jet, and electrohydrodynamic jet printing constitute three distinct technologies for precise patterning of functional materials in an additive, digital, and noncontact manner. While the unique physical mechanism of each technology endows it with specific advantages and disadvantages, commonalities in materials compatibility, patterning capabilities, and application domains motivate a holistic assessment of nanomaterial integration with these methods. This report will highlight progress across ink formulation, process design, and application development from recent years, with an emphasis on emerging materials and practical applications in this evolving field of research. This includes an overview of the three printing technologies, a survey of ink formulation and printing efforts across conductive, insulating, and semiconducting materials, an examination of compelling application demonstrations in electronics, sensing, and energy, as well as discussion of key emerging themes related to artificial intelligence, multimaterial printing, and nonplanar patterning.

1. Introduction

1.1. Overview

Digital printing technologies offer a versatile platform for advanced manufacturing of functional devices and systems. Among this broad scope of methods, droplet-based material jetting provides a compelling combination of material compatibility, high resolution, and non-contact deposition. By precisely dispensing liquid inks formulated with functional nanomaterials, coordinated with a computer-controlled motion platform, these techniques allow fabrication of microscale systems, with electronic functionality being a primary target.[1,2] Here, we focus explicitly on three widely adopted, versatile printing methods that exhibit similarities in materials compatibility, application fit, and qualitative process descriptors: inkjet,[3] aerosol jet,[4] and electrohydrodynamic (EHD) jet printing.[5] The inherently digital nature of these technologies accelerates research and prototyping, and provides unique opportunities for versatile fabrication of flexible, hybrid, and conformal devices. A cornerstone of this vision is the ability to adapt a wide range of functional materials to a narrow set of deposition methods. This requires formulation of nanomaterial inks as a foundational pillar of this field. While digital printing of nanomaterial inks offers significant potential beyond electronics, the evolution of this field has been nearly synonymous with printed electronics to date, and thus many applications highlighted here are centered on electronic functionality.

1.2. Motivating applications

There are widespread application opportunities for digital printing of nanomaterials in electronics, spanning displays,[6] flexible circuits,[7] electronics packaging,[8] communication,[9] energy,[10] and sensing,[11] among others (**Figure 1**). While the diversity of device demonstrations exhibited within the academic literature is vast, this is not a comprehensive review of printed devices. We instead focus on a subset chosen based on fit between the chosen application and the printing methodology, practical relevance on a moderate time horizon, and generality.

While arguably not the most glamorous application, a broad and impactful need for nanomaterial inks is for patterning of conductive wires for basic circuitry. Comparable to wiring of printed circuit boards, power and signal connections that can be adapted to flexible, conformal, or large-area surfaces have widespread application. For multilayer circuitry, this requires insulating layers to form signal crossovers, and functionality of the conductor encompasses electrical conductivity, print resolution, and print aspect ratio. This drives a large, established market for conductive inks.[12] While this spans high throughput patterning methods (i.e., screen, gravure, flexographic printing), digital droplet-based methods offer excellent precision, improved research and prototyping characteristics, and unmatched agility. For single-layer printing on a flat surface, the case for droplet-based methods is more challenging to make outside of prototyping; for multi-layer printing that requires registration to underlying features, the ability to adapt on the fly is a key strength. Moreover, extension to conformal patterning on 3D surfaces enables an application space with limited competition,[13–16] particularly for broad materials.[17,18]

Iowa State University, Ames, IA, USA 50011.
* Corresponding author: esecor@iastate.edu

View Article Online
DOI: 10.1039/D5NR02110C

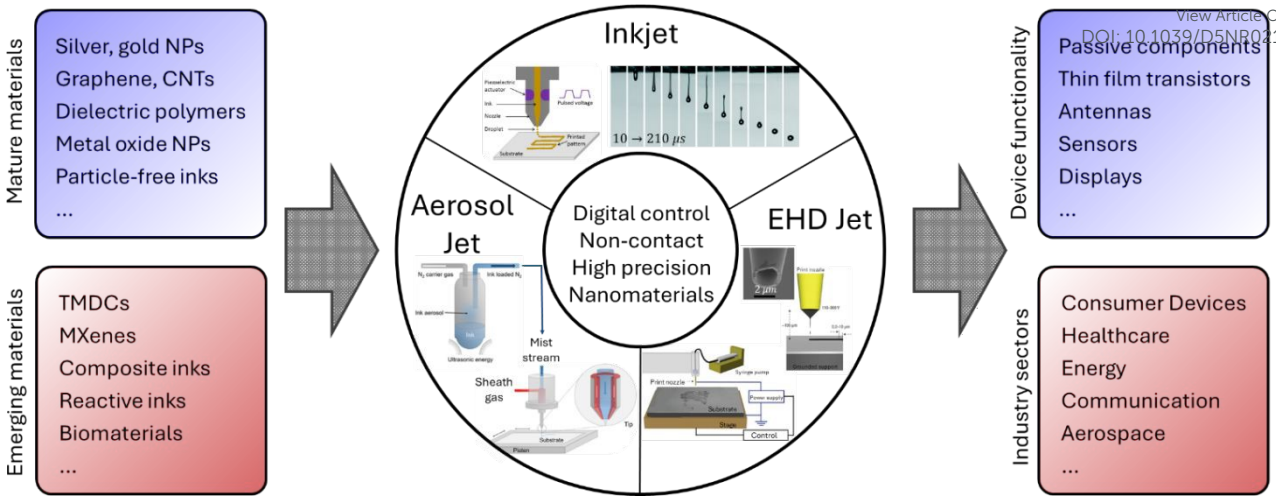

Figure 1. Overview of droplet-based printing technologies for functional devices. Inkjet, aerosol jet, and EHD jet printing are the focus of this report, given their high-level similarities in materials requirements and process integration characteristics. Graphics adapted with permission from Ref. 14, 15 (CC BY), 16, and 179 (Copyright 2009 American Chemical Society).

A second broad application area is encompassed by hybrid electronics – the combination of conventional microelectronics technologies with printed components.[19,20] At one end of this spectrum, this can describe electrical connections to discrete passive or active devices, such as resistors and capacitors, paralleling the functionality of printed circuit boards but with some capability to generalize. In higher precision embodiments, this is exemplified by interconnects to bare die, such as replacing wire bonds,[21] along with emerging interest for heterogeneous integration and advanced packaging.[22,23]

For the previously mentioned application areas, the basic requirement to print metal and dielectric structures with high geometric precision and material quality is the core foundational technology. As more diverse functionality is added, the application potential for these methods broadens significantly. Two areas in particular include active electronics for logic, with the core unit being the thin film transistor,[24] and sensing, which can describe a wide range of transduction mechanisms and target analytes.[25–27] While printed transistors will not be competitive with conventional microelectronics in terms of performance, reliability, integration density, and power, they can provide a compelling fit for applications requiring low integration density – i.e., a relatively small number of transistors distributed over a large area. Backplanes for display technologies are a prime example,[28,29] and more generally such functionality could support some level of signal conditioning or edge computing.[30] Sensing, encompassing mechanical, chemical, electromagnetic, and other stimuli, is a diverse application space with significant opportunities for printing technologies. More than any other application discussed here, this benefits from the functional diversity of printable materials and often fits the low volume, high mix production aligned with digital manufacturing.

These benchmark applications shape the development of nanomaterial inks. Conductive inks are a workhorse for the broad scope of electronics applications, with silver currently the most prevalent material, but needs for alternative metal and non-metal inks for specific features.[30–32] Dielectric inks compose a second broad class defined by electronic functionality, and while crucial for practical applications, these have not benefited from the same level of research and development in recent years.[33] The last major class comprises semiconducting inks,[34] which augment the diversity of materials and applications by enabling active logic, optoelectronics, expanded sensing functionality, and other benefits.

1.3. Organization and scope

This report focuses on nanomaterial inks for droplet-based digital printing methods, with particular emphasis on inkjet, aerosol jet, and EHD jet printing. While printed electronics is a relatively mature field, advances in materials and processing methods continue to expand the capabilities and application space of these technologies. In the context of functional devices, all three methods share similar requirements for materials chemistry and dispersion quality, and similar considerations for applications, thus motivating their collective analysis. For this review, we survey different elements of printed electronics and discuss recent and emerging trends shaping the evolution of this field. We introduce the three printing technologies to highlight characteristics of the processing platform that constrain and guide ink formulation. We then focus on inks, broadly categorized based on electronic functionality due to the preponderance of practical applications in this domain, concentrating on recent research advances within the context of longer-term developments. We briefly overview post-processing, followed by a discussion of selected exemplary application demonstrations. Finally, we provide a perspective on the outlook of this field moving forward, including emerging trends and opportunities that span integrating increasingly sophisticated digital capabilities, bottom-up multimaterial patterning, and more complex 3D geometries. This review is not comprehensive, and many compelling and noteworthy demonstrations and developments are surely overlooked, but the aim is to provide a broad outlook on this field to accessibly contextualize materials, printing, post-processing, and applications.

View Article Online
DOI: 10.1039/D5NR02110C

2. Droplet-Based Digital Printing Technologies

2.1. Parallels in droplet jetting methods

As a class of printing technologies, inkjet, aerosol jet, and EHD jet printing provide compelling capabilities for patterning functional materials (**Figure 2**). Relative to the broader scope of patterning technologies, these feature several core commonalities. First, they are liquid-phase, relying on functional inks, and each relies on droplet formation for patterning, which places constraints on particle size, fluid properties, and patterning configuration. To enable liquid-phase printing, active materials in the form of nanoscale or molecular species are formulated as inks and patterned, then often post-processed to return some semblance of bulk material properties. This contrasts with a number of melt-phase, powder-based, or electrochemical additive methods, but supports considerable versatility in the functionality of materials by placing the burden for developing compatible materials first and foremost on ink formulation.

Alongside the bottom-up requirements based on process science, these three jetting technologies occupy a similar space in terms of attributes and applications. In short, these methods are digital, non-contact, and high resolution. *Digital:* All three are digital patterning methods, meaning the target pattern to fabricate is embedded in a digital format and executed by a computer-controlled printing system. This is of course advantageous for research and prototyping environments, for which continuous modification of printed patterns supports rapid refinement of designs and process parameters. This also facilitates operation in less conventional modes, such as additive repair,[35] that must be responsive to the actual geometry of the substrate or pre-existing patterns. In the same way, digital methods can serve an important role for multi-layer patterning.[36] Rather than propagating and amplifying errors in lower-level patterns, these digital techniques could detect and accommodate such errors to provide a more robust and resilient manufacturing process. *Non-contact:* By depositing small droplets onto a surface from some meaningful standoff distance, these three jetting methods allow patterning within new constraints. Printing on sensitive surfaces becomes feasible, such as biological or deformable substrates. In addition, these methods allow more straightforward printing on complex 3D surfaces compared to most contact-based methods, with the standoff distance providing some tolerance for accurately contouring the 3D surface.[37] *High resolution:* Print resolution is a primary metric that defines the suitable application space of a given technology. While there are differences across these three methods, they all span ~100 nm – 100 µm size range for the 'unit' process, i.e., a single printed droplet or line. This is a promising size range for relevance in electronics packaging and board-level circuitry.

These similar attributes lead to broad similarities in materials development, allowing a cohesive overview. While there are methods that serve similar applications – i.e., transfer-based printing methods, extrusion printing, and screen printing – these do not share enough similarities in fundamental physics or technological attributes to justify inclusion here. One common method that is omitted, in particular, is direct ink writing or extrusion printing.[38] While many qualitative applications are similar, the wide range of nozzle size for DIW allows micron-scale particles, while the close proximity of the print nozzle and surface put it in an ambiguous realm regarding contact vs. non-contact deposition.

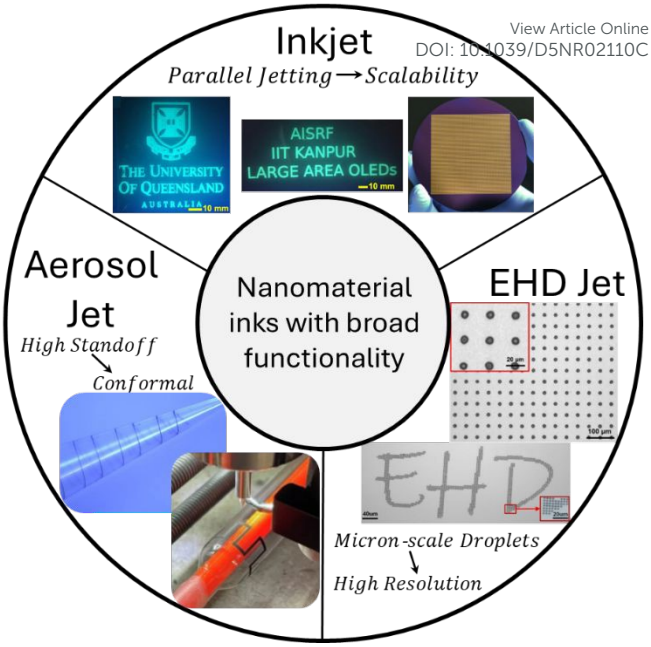

Figure 2. Key droplet-based printing technologies and their distinguishing benefits. Graphics adapted with permission from Ref 39 (CC BY), 70, 176 (CC BY), and 280 (CC BY-NC-ND).

The three methods are distinguished by their droplet generation and deposition mechanisms. While this imposes differences on how inks are tuned for the individual methods, and what features, advantages, and disadvantages characterize each, broadly speaking the generation and deposition of fine droplets to pattern materials leads to commonalities in materials compatibility, downstream processing, and applications. For each of the three printing technologies discussed, we will introduce the method and provide broader context, and then discuss the mechanism of the process, typical patterning metrics, benefits and drawbacks, and several illustrative use cases.

2.2. Inkjet Printing

The most broadly adopted of the three, inkjet printing has a long history in the graphic arts industry prior to being adapted for functional materials around the 1990s. Given this history, inkjet printing is the most mature of these methods, and serves as a useful benchmark. While historically there have been variations of inkjet printing based on bubble generation (thermal inkjet printing, or bubble-jet printing) or leading to continuous droplet production, the most common platform for functional device fabrication is drop-on-demand piezoelectric inkjet printing. In this implementation, a MEMS printhead contains an array of nozzles that are actuated by a piezoelectric transducer. Careful control over the electrical signal fed into the transducer – the waveform – allows for generation of a pressure

wave that optimally leads to ejection of a single droplet through a narrow orifice or nozzle. The nozzle size can range from ~50 µm down to ~10 µm, defining droplet volumes from ~100 pL to ~1 pL. By synchronizing the actuation of individual nozzles with the motion of the printhead across a substrate, patterns can be produced with many nozzles operating in parallel. Many lab-based demonstrations use printer cartridges with 1-16 nozzles, but commercial printheads can scale this to 1024 or more individual nozzles. Because of this, inkjet printing has the greatest range in the tradeoff of throughput and resolution among droplet-based printing methods, offering a compelling advantage for transitioning from research and development to production (**Table 1**).[39]

Ink formulation for inkjet printing is driven by three key requirements: engineering for suitable jetting, wetting, and drying. Jetting criteria are well established based on fluid dynamics and are captured by nondimensional numbers related to droplet formation. In particular, the inverse Ohnesorge number is frequently used to screen materials for jettability, identifying a suitable viscosity range and, to a lesser extent, surface tension, while considering the nozzle size.[40] Excessively viscous inks prevent droplet formation by dissipating the pressure wave within the fluid, while overly inviscid inks can lead to satellite droplet formation and an accompanying deterioration in print quality.[41] Wetting describes how droplets spread and coalesce with neighboring droplets on a substrate. As with jetting, there is a balance to achieve here. Excessive wetting reduces precision and can lead to nonuniform deposition of material, while insufficient wetting can prevent formation of continuous lines and films or lead to unstable liquid migration on the surface. As opposed to jetting, which is primarily contingent on the interplay of the ink and the printer, wetting is dictated by the interaction of the ink and the substrate surface. Both surface energy and surface roughness have a role, along with the surface tension of the ink. It is common to qualitatively assess wetting characteristics by measuring the ink contact angle on the surface, although this is typically a static contact angle and not wholly representative of dynamic phenomena. Importantly, nanomaterial inks will typically exhibit some degree of contact line pinning arising from deposition of functional materials, leading to a quasi-stable contact line.[42] This behavior is challenging to predict and quantitatively assess, but can often be initiated via ink binders.

Drying is the final stage of patterning, before any post-processing. Because liquid inks commonly contain a high-volume percentage of solvent, this carrier fluid must be removed by evaporation to yield a solid deposit (many UV curable inks are an exception to this statement but are less representative of typical nanomaterial formulations). Evaporation of solvent from the fluid bead leads to internal temperature and composition gradients that drive transport. This can cause the functional material to deposit near the periphery of the droplet/feature, in what is known as the coffee ring effect.[43] Manipulation of the ink, surface, and drying environment can mitigate or reverse this effect, with significant impacts on the uniformity of printed material.[44,45] For some applications, controlling this stage of the process is critical, and less straightforward than the relatively explicit criteria required for droplet formation. Coffee ring formation has also been deliberately exacerbated and exploited for several laboratory demonstrations,[46–48] although the preponderance of applications require reduction in this effect to improve uniformity.

Table 1. Overview of typical parameters for common droplet-jetting printing technologies

	Inkjet	Aerosol Jet	EHD Jet
Resolution	20-100 µm	10-100 µm	0.1-100 µm
Viscosity	1-20 mPa-s	0.5-1000* mPa-s	0.5-10000 mPa-s
Dominant fluid characteristics	Surface tension, viscosity	Viscosity, vapor pressure, surface tension	Surface tension, electrical conductivity, viscosity
Advantages	Parallel operation (throughput), technological maturity	High standoff distance, limited nozzle clogging	High resolution, high viscosity range
Challenges	Nozzle clogging, narrow viscosity range	Overspray	Standoff distance, print throughput

*Approx. 0.5-10 mPa-s suitable for ultrasonic atomization, with higher range possible using pneumatic atomization for droplet generation

One of the limitations for inkjet printing is in scaling to smaller feature size. While this is not a hard constraint, as the production of finer nozzles is certainly feasible, the physics of the process becomes more demanding at smaller length scales. On one hand, particles with finite size can affect the propagation of pressure waves through the ink in the droplet formation step and can also physically clog the nozzle when they are on a similar order of magnitude in size scale. In addition, the energy required to form droplets, effectively overcoming surface tension, exhibits a relative increase when moving to smaller dimensions. If the print resolution is constrained primarily by the droplet size, and this is dependent on the nozzle size, this establishes a constraint to scaling to finer and finer features.

2.3. Aerosol Jet Printing

Aerosol jet printing (AJP) was originally developed by Optomec, Inc. as part of the DARPA MICE program in the late 1990s and early 2000s. Early work in academic labs, including efforts by Frisbie, et al., helped popularize this method and increase its adoption in the materials research field.[49] In a sense, AJP decouples the critical tasks of droplet generation and droplet patterning, printing a polydisperse mist of micron-scale aerosol droplets with bulk aerodynamic controls rather than generating and controlling individual droplets directly. During the process, droplets are formed in an atomizer using either ultrasonic or pneumatic methods. These droplets are suspended in a carrier gas flow and transported to the printhead, where an annular

View Article Online
DOI: 10.1039/D5NR02110C

sheath gas surrounds the aerosol stream as it moves through a fine nozzle and is deposited on a substrate.[50]

The stages of aerosol jet printing differ from inkjet printing in that droplet generation, transport, and deposition are largely decoupled; wetting and drying phenomena, meanwhile, parallel those for inkjet printing with some notable differences. Droplet generation for aerosol jet printing is less controlled and precise than for other droplet-based printing methods, in that the process can tolerate a polydisperse distribution of aerosol droplets. With ultrasonic atomization, the classical understanding of droplet formation is based on pinch-off from a standing capillary wave on the liquid surface, in which the droplet size is largely based on the surface tension and ultrasonic frequency, and droplet generation is limited by viscous damping of the acoustic energy that imparts an upper limit on ink viscosity.[51,52] More viscous inks, therefore, rely on pneumatic atomization, in which high velocity two-phase (ink and carrier gas) flow through a narrow orifice result in liquid sheets and jet break-up and the generation of a wide distribution of droplet sizes. Much of the complexity of this process is covered over, as large droplets are collected within the cartridge, moderate-sized droplets settle out gravitationally before they reach the printhead, and very small droplets can be removed via a virtual impactor, which has the important purpose of reducing the gas flow rate.

Within the printhead, the sheath gas prevents droplets from impinging on the interior surface of the nozzle, helping prevent clogging and allowing feature sizes much smaller than the nozzle dimensions (i.e., 10-40%). This sheath gas also has an important influence on the droplet composition, as a dry sheath gas induces evaporation of solvents in the inks.[53,54] This has the upside of increasing fluid viscosity and decreasing solvent volume prior to droplet impact on the surface, which can reduce liquid-phase spreading and improve stability of printed features.[55] It also has a downside, in that the reduction in droplet size, and thus inertia, that results from evaporation on the periphery of the aerosol stream contributes meaningfully to overspray, a characteristic of AJP that describes diffuse deposition of material along the edges of printed patterns.[56]

These two mechanisms – droplet formation, and droplet evaporation within the printhead – constrain and guide ink formulation. The requirement for droplet formation limits ink viscosity, particularly for ultrasonic atomization, and constrains the particle size as well. The drying action of the sheath gas constrains the vapor pressure of ink solvents, with excessively dry (high vapor pressure) inks resulting in significant overspray and granular morphology, and excessively wet (low vapor pressure) inks resulting in liquid-phase spreading, which can become uncontrolled under the high velocity gas jet. As implied above, this in-line drying modulates the influence of wetting and drying mechanisms that have been previously discussed in the context of inkjet printing.

Continuing efforts to improve AJP capabilities have in many cases focused on fine line patterning. While resolution in the 10-50 µm range is reasonably achievable, this 10 µm threshold has recently been exceeded through rigorous process optimization,[57,58] along with creative strategies to exploit non-aerodynamic focusing via acoustic fields.[59,60] These demonstrate that 10 µm is not a fundamental limit, and generalizing these results to broad material sets and higher deposition rates will further expand the capabilities readily accessible to AJP technology.

2.4. Electrohydrodynamic Printing

EHD jet printing has been gaining popularity in research and development, principally within the scope of printed electronics. It offers excellent potential for high resolution patterning, reaching sub-micron feature size.[61] Implementations of electric field-driven fluid patterning have a long history (>150 yrs), and modern EHD jet printing is supported by the theory developed by Taylor on electrostatic droplet generation from fluids. Over the past ~25 years, this has evolved into a sophisticated technology for material patterning, beginning largely with droplet arrays and organic materials. The work of Rogers, et al. helped popularize the method for electronics, owing to the step change e-jet printing offered in feature resolution compared to traditional inkjet printing methods, along with distinct fluid requirements.[5,61–63]

During EHD jet printing, the functional ink is passed through a charged nozzle, which forms a closed circuit with the substrate. The electric field between the nozzle and substrate causes charge build-up on the fluid surface, which deforms to create a Taylor cone. At suitable conditions of liquid back-pressure, material properties, and electric field, the liquid can form a stable cone jet, resulting in break-off of very fine (~fL) droplets which then deposit on the substrate surface. Different jetting modes are possible, and application of a pulsed electric field to induce droplet formation can offer better control of frequency and droplet size.[64] It is also possible to use alternating current to address challenges of residual charge buildup for inks on insulating substrates.[65] Given the mechanism of droplet formation – relying on an electrical field to pull off droplets rather than a pressure wave to eject material – the requirements for ink formulation are quite distinct from traditional inkjet printing. With droplet formation being driven primarily by competition between surface tension and electrostatic phenomena, electrical conductivity and dielectric permittivity of the ink are important properties, alongside surface tension. Viscosity remains important as a secondary variable, implying a wide range of viscosities can be effectively printed but that higher viscosity inks can influence dynamics of droplet formation and the relaxation timescale of the ink.[66] Additives can be incorporated in inks to modulate surface tension, electrical conductivity, and viscosity to tailor characteristics for EHD jet printing. Alongside the material properties, printer system characteristics including nozzle size and surface characteristics, nozzle-substrate distance, and voltage are significant determinants of the print capability and quality.[67]

Following deposition on the substrate, the wetting and drying characteristics of EHD jet printing parallel those for inkjet and aerosol jet. While electrostatic repulsion in the charged droplet can result in somewhat lower contact angle and large

View Article Online DOI: 10.1039/D5NR02110C

wetting radius, this is a modest effect in comparison to the substantially reduced droplet volume compared to other droplet-based printing methods. As with AJP, EHD jet printing employs droplets much smaller than the nozzle size. While this can aid in reducing nozzle clogging, it does not entirely eliminate it. Solvents with moderately high boiling point, and small particle size with high dispersion quality, remain effective for mitigating nozzle clogging during printing.

Based on its unique physics, EHD jet printing has significant benefits for high resolution patterning.[67] The flip side of this is a reduced print throughput, given the frequent use of single-nozzle printing, extremely fine droplet size, and physical limitations in the jetting frequency. Moreover, because e-jet printing is driven by an electric field between the nozzle and substrate, it is poorly equipped to accommodate a high amount of roughness, nonuniformity, or 3D topography in surfaces.[68] Novel approaches to EHD jet printing continue to be introduced, including methods potentially suited for patterning on curved surfaces by exploiting surface polarization,[69] along with strategies to dramatically increase jetting frequency.[70]

3. Nanomaterial Inks

3.1. Conductors

Silver nanoparticle inks are widely used for high resolution printing because of their high electrical conductivity, modest sintering requirements, and processing tolerance. They offer good adhesion to a number of substrates while being adaptable to different printing methods.[71] Traditional silver nanoparticle inks contain surfactants or polymer dispersants, which support colloidal stability by coating the particles' surface. This leads to a barrier between particles following deposition and drying, often necessitating curing to support high electrical conductivity. This sintering step is a focus of research in silver nanoparticle ink development and processing, as low-temperature sintering can reduce energy requirements and expand the scope of compatible substrates. In addition, while a wide range of silver nanoparticle inks are available commercially, recent research continues to explore alternative methods for ink development that mitigate cost and environmental concerns,[72] or to support custom characteristics. For example, algal and microbial extracts have been demonstrated for synthesis of silver nanoparticles with less reliance on traditional chemical synthesis.[73] Custom-made inks to support thermally sensitive substates are a key focus, targeting compatibility with low temperature or thermal sintering methods. For example, electrolytes containing chlorine anions have been added to inks to support aggregation and coalescence of silver nanoparticles.[74,75]

Custom inks also provide an opportunity to tailor nanomaterial morphology for custom functionality. While silver nanoparticles are effective for reasonably dense, conductive lines, they form optically opaque patterns. Silver nanowires, on the other hand, can form sparse percolation networks to support both electrical conductivity and optical transparency for use as a transparent conductor. For example, a custom silver nanowire ink was synthesized with silver nitrate, polyvinylpyrrolidone, and ethylene glycol, and by controlling the nanowire length, the authors were able to formulate an ink compatible with inkjet deposition using a desktop printing system.[76] More generally, silver nanowires are considered for applications in microelectronics, thin-film solar cells, and biosensors.[77–80] For these 1D nanomaterials, there is a general tradeoff in the morphology and printing performance, with high aspect ratio desired for efficient percolation to support transparent conductors but making inks more prone to droplet formation difficulties, limited solids concentration, and complex rheology.[76]

Although silver is extensively used for fabricating electronics and prototypes, in general the materials research community has shifted to other printed conductors given the maturity of commercial silver inks (**Figure 3**). With silver as the benchmark, these other materials must demonstrate some realistic advantage on at least one dimension to justify development. While not an exhaustive list, we will highlight here recent

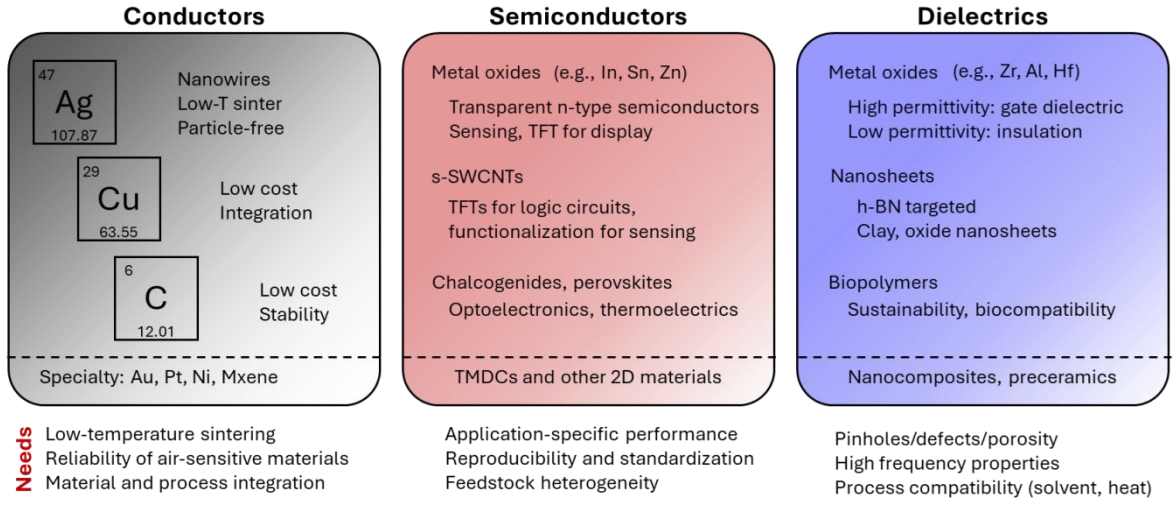

Figure 3. Overview of common materials and classification for droplet-based printing technologies focused on electronic characteristics.

View Article Online
DOI: 10.1039/D5NR02110G

research efforts focused on other metals, along with select inorganic conductors beyond traditional metals.

Gold is among the more established materials for nanoparticle inks beyond silver given its historical importance in nanotechnology and tolerant synthesis and processing. For applications, the primary benefits that gold offers include its extreme resistance to oxidation and its biocompatibility. Of course, the cost of gold is substantially higher than that of silver, so significant benefit must be justified for this to be a logical replacement for silver. Because of its higher melting point, gold nanoparticle inks in many cases exhibit higher sintering temperatures than necessary for silver. A notable recent effort to develop low-temperature sintering gold inks compatible with both inkjet and aerosol jet printing resulted in resolutions less than 20 μm while achieving electrical resistivity as low as 9.6×10^{-8} Ω·m for 400 nm thick films.[81,82]

Zinc is an alternative conductive material with unique characteristics for biocompatibility and biodegradability. However, the printing and sintering approach for zinc is generally quite distinct from traditional silver nanoparticle inks due to the ready oxidation of nanoscale zinc particles. Majee et al. printed a zinc nanoparticle ink made from glycols (i.e., dipropylene and ethylene) and polyvinyl butyral through inkjet on a polyethylene terephthalate (PET) substrate. Thereafter, the printed patterns were chemically sintered using acetic acid. Such a method removes the need for thermal sintering and thus allows integration with thermally sensitive substrates and other materials, in this case yielding conductivities on the order of 10^5 S/m.[83] Furthermore, although inks made from zinc may act as alternative conductors to silver, they also hold promise for printed primary batteries, and zinc's biodegradability aligns with opportunities for transient electronics.[84–86]

Coppers inks have been a significant focus for fundamental and applied research in printed electronics for years. The most commonly cited driver for this is cost and abundance, and copper offers comparable electrical conductivity to silver. In addition, copper is a benchmark material for printed circuit boards and microelectronics, and so many peripheral materials and methods – for example, solders – have been developed to be compatible with copper. In some cases, printed silver is not an effective drop-in replacement within this larger processing environment. While some commercial distributors of copper inks exist, the technical challenges and broad potential for this material motivate continued research efforts. In particular, while bulk copper has high conductivity, nanoparticle-derived films typically exhibit significant porosity, and the high surface area and curvature of such films make them prone to oxidation. While films derived from silver nanoparticles are tolerant to this – they have a higher reduction potential than copper and remain conductive in the oxidized state – copper has proven to be much more sensitive. This can lead to both immediate effects (significantly greater challenges in achieving conductivity comparable to bulk), and long term stability concerns.[87] Such instability can reduce the electrical conductivity of copper prints and hamper reliability in applications. For this reason, some researchers have employed strategies to maintain good conductivity while curbing the problem of instability. One example is the core-shell approach, in which a layer of oxidation-resistant material covers a copper core within each nanoparticle.[88] The use of capping agents in copper ink formulation also has a significant role for oxidation stability, forming a barrier between the copper particle and the outside environment to slow down the oxidation process prior to printing.[89–92]

Apart from pure copper conductive inks, inks made of copper alloys can find application in sensing systems, such as CuNi for thermocouples. For these applications, reduced electrical conductivity compared to bulk is not a strong performance driver, so this can be more tolerant to the challenges with oxidation and porosity. Several researchers have therefore demonstrated printing of such alloys. Gu, et al. made a printable, aqueous, oxidation-resistant constantan ink using polyvinyl pyrrolidone, ammonium chloride and glycerol, from which a sensor was fabricated via inkjet printing, yielding a temperature coefficient of resistance of 4×10^{-5} K^{-1}.[93] Sheng, et al. featured a thermocouple made of Cu-CuNi nanoparticle ink and printed via inkjet deposition. It showed high sensitivity (20.6 μV/°C) while maintaining stability under thermal cycling.[94] Likewise, a temperature sensor of high sensitivity (~40 μV/°C) was fabricated via aerosol jet printing using Cu and CuNi inks.[95]

Among other conductors, platinum is an expensive material like gold, but one with exceptional properties for certain high value applications. Having a high melting point, broad catalytic activity, biocompatibility,[96] and electrochemical stability, platinum has been explored for fuel cells,[97] dye-sensitized solar cells,[98] electrochemical sensors,[99] and high temperature electronics.[100] Platinum inks can include both particle-free and colloidal formulations, given the high redox potential of platinum.[100,101] Nickel inks can be magnetized and withstand high temperature oxidizing environments.[102] It has been shown that nickel ink made from nickel acetate, polyvinyl pyrrolidone and ethylene glycol is compatible with aerosol jet printing on various substrates for high temperature applications.[102] Apart from the coinage metals, a titanium-based ink in the form of hydride nanoparticles has also been demonstrated for aerosol jet printing, representing an alternative approach.[103]

In a broad sense, metal inks are commonly used for their high electrical conductivity. However, issues such as cost (silver, gold, platinum), oxidation susceptibility (e.g., copper), high sintering temperatures, and concerns of toxicity have motivated the development of alternative conductive inks. In this regard, graphene- and MXene-based inks have been extensively developed for various printing technologies. Because the latter are described thoroughly in recent review articles,[104–106] we limit the discussion here, but MXene inks have been demonstrated for inkjet, EHD, and aerosol jet patterning technologies, with applications including electrochemical energy storage and sensing.[107–109] The ability to form stable, dispersant-free formulations of MXenes significantly aids in obtaining highly conductive patterns with low processing temperature, and tailoring ligand chemistry can further support solvent versatility.[110]

Both graphene and MXene printed materials are composed of high aspect ratio flakes or platelets, which allow fairly dense

film packing. Macroscale functionality of such printed patterns are based on both the material properties of individual flakes and, crucially, the flake-to-flake interconnections.[111] As another point of commonality, these materials do not sinter in the traditional sense, such that the flake-to-flake junction resistance can be meaningful. As a result, printed conductors often favor larger particle sizes for electrical functionality, but this can come at a tradeoff for dispersion quality, solids loading, and ease of printing due to rheological effects of high aspect ratio particles and size limitations where dispersed particles begin to influence droplet formation physics.[112]

Graphene is touted to have good mechanical strength, thermal stability, and electrical properties.[113,114] However, there is a wide range of achieved conductivity for printed graphene in various works, ranging from <300 to 7.13×10^4 S/m.[115–118] This variation may be in part attributed to the quality of graphene produced for inks, related to flake size, defect density, and heteroatom content, along with flake-to-flake interconnections. While there are a variety of uses for printed graphene, in many cases the target is either high conductivity or electrochemical activity, and the target graphene properties can thus vary depending on the application.

For highly conductive printed patterns, low defect density, low heteroatom content, and large flake size is usually a preference.[119] In developing graphene inks, issues related to particle aggregation must be carefully addressed to ensure favorable and stable deposition.[120] This often requires dispersants or stabilizing agents, which influence electrical conductivity and required post-processing steps.[121] To achieve low processing temperature, it is preferred to limit the use of such stabilizing agents or eliminate them altogether, but this must ideally be achieved without compromising good dispersion of the ink.[122]

In addition to its use for conducting patterns,[123] graphene offers a high surface area due to its 2D structure, and can contain chemically active sites in the case of oxidized materials.[124] It is therefore capable of chemically interacting with molecules as well as facilitating carrier transport.[125,126] These interactions can thus be harnessed in the area of electrochemical devices for sensing and energy storage.[127,128] While the electrical conductivity remains relevant for these applications, in many cases it is outweighed by surface area and electrochemical considerations, with an inherent tradeoff between highly active, poorly stacked materials for electrochemical activity and densely stacked, highly pure materials for electrical conductivity and electrochemical inertness.

3.2. Dielectrics

One benefit of the printing technologies discussed here is their versatility for patterning disparate material classes. This contrasts with many additive manufacturing methods that are designed for a single type of material, such as metals, UV-curable polymers, or thermoplastics. Aside from conductive materials, inks containing dielectric materials can be printed for numerous purposes; they are notable for passive electronic devices such as capacitors,[129] find wide applications as an insulating material in general electronic packaging,[130] and are a crucial element for active devices such as transistors and certain types of sensors. In some cases, the particular application drives the choice of dielectric material based on material properties such as dielectric constant, breakdown strength, thermal stability, and film microstructure. The dielectric constant, or relative permittivity, is a useful measure to help classify different printed materials, with high dielectric constant useful for capacitive coupling (transistor gates, capacitors),[131] while low dielectric constant is generally preferred for insulating characteristics.[130]

A common device that relies on dielectrics is the thin-film transistor (TFT), a basic building block for more complex electronic circuits. Here, the dielectric couples a gate bias into the active semiconducting channel to modulate charge transport while maintaining minimal leakage current through this gate dielectric. For this application, high capacitance is preferred to reduce the working voltage of the device. For printed TFTs, the gate dielectric must also withstand subsequent processing steps, which could include solvent and thermal exposure, while maintaining a pinhole-free barrier. High-k metal oxide dielectrics are a common target for this application, including compositions based on molecular precursors of alumina, zirconia, and hafnia to achieve thin, smooth, amorphous films.[132–136] A common challenge for these materials is the traditionally high processing temperature required to achieve dense, pinhole-free films with suitable dielectric characteristics. Sol-gel processing for metal oxide thin films traditionally requires temperatures exceeding 400 °C, which are incompatible with flexible substrates. Strategies to alleviate these concerns include alternative annealing methods such as intense pulsed light and deep UV exposure,[137,138] along with tailoring chemical precursors to generate heat during exothermic decomposition and overcome the energy barrier for conversion to oxides with less external heating.[139] A recent example used a solution-processable aluminum oxide film annealed by intense pulse light for the gate dielectric of a metal oxide transistor, which showed a large capacitance of 109 nF cm^{-2} and low leakage current density of $<10^{-8}$ A cm^{-2} at a working voltage of 10 V.[140] Achieving thin, pinhole-free films for transistors remains a challenge, particularly for high purity dielectric materials that can support high frequency operation with minimal loss.

While sol-gel methods can yield dense dielectric films, nanomaterial-based dielectrics can also be employed in certain applications. In particular, 2D nanomaterials can exhibit favorable film morphology to support electrical isolation. An example within this category is hexagonal boron nitride. With a bandgap of 6 eV, chemical and thermal stability, high mechanical strength, and a basal plane free of dangling bonds, boron nitride is a promising dielectric for electronics.[141] However, as with graphene, the material quality achieved for printed devices significantly lags that for single-flake demonstrations. Liquid phase exfoliation of bulk hexagonal boron nitride flakes has been employed for ink preparation, with additional stabilization methods to reduce aggregation and

View Article Online
DOI: 10.1039/D5NR02110C

support printing of thin, pinhole-free films.[142] In contrast to the low dielectric constant of boron nitride, researchers have synthesized high dielectric constant (k~192) perovskite nanosheets, such as $Ca_2NaNb_4O_{13}$. By printing single and multilayer devices using this family of nanosheets, Zhang, et al. demonstrated fully-printed capacitors with a capacitance density as high as 346 nF cm^{-2}.[143,144]

Polymer dielectrics provide distinct processing and performance characteristics compared to most inorganic printed materials. In general, they offer better process compatibility at low temperature, at the tradeoff of limited thermal stability. While often the thermal stability is sufficient for applications, it restricts subsequent process steps, such as sintering metal nanoparticle inks. While this report overall is largely focused on inorganic materials, within the scope of dielectric materials the use of nanocomposites can provide an effective means to tailor properties while leveraging the inherent properties of inorganic materials. For example, Wu, et al. developed a nanocomposite dielectric ink based on nanosheets of $Ca_2Nb_3O_{10}$ in a PMMA matrix.[145] This ink was patterned by aerosol jet printing to form the gate dielectric for a thin film transistor. In the same way, Abdolmaleki, et al. demonstrated inkjet printing of a $BaTiO_3$/PVDF ink.[146] Here, the $BaTiO_3$ affected the crystallinity of the PVDF to enhance ferroelectric and piezoelectric characteristics. In addition, a $Ba_xSr_{1-x}TiO_3$/PMMA ink for inkjet printed capacitors exhibited high dielectric constant of 20-42 at 1kHz.[147] Such composites harness the low temperature processing and flexibility of polymers while leveraging inorganic nanomaterials to tailor performance.

Although some studies have been done to utilize composite dielectric inks for inkjet[148] and aerosol jet[130] techniques, in general dielectric materials are lagging conductors in their development for non-contact printing methods, and clear standards and performance criteria would aid broad development in this space. While conductive materials have relatively explicit and easy to measure metrics, dielectric performance can often be context-dependent and relate to pinholes, reliability, stability to subsequent processing steps, and other factors that are more challenging to generalize.

Irrespective of application or dielectric type, a quality of critical importance in printing dielectric inks is the homogeneity of the print, as this directly influences device performance characteristics such as insulator performance, consistency, and reliability.[149,150] Thus, careful attention must be given to both ink engineering and printing parameters to achieve uniform deposition. Here, there is significant work required to better understand how material development and process design intersect to influence tradeoffs in patterning resolution, uniformity, and microstructural quality.

3.3. Semiconductors

The last major material class for printed electronics within scope of this effort is semiconductors. While there remains need for printed semiconductors in benchmark logic devices, such as TFTs, there is significant need for bespoke material solutions for much broader applications, such as sensing, where the material versatility and prototyping capability of printing methods provides a clear benefit. For large-area patterning, such as backplanes for displays, printing methods do align with the form factor and resolution requirements to provide a feasible and practical solution. For high performance logic traditionally done with microelectronics, there is limited motivation to replace conventional silicon with printed devices that are much larger, lower performance, variable, and less reliable. As a result of the disparate application spaces for printed semiconductors writ large, it is challenging to define explicit performance criteria to evaluate different material solutions. The discussion here will focus on several key areas – carbon nanomaterials for flexible logic devices, metal oxide semiconductors primarily for display applications, and chalcogenide materials for optoelectronics, which cover a limited space of printed semiconductors.[151–154]

Because of their flexibility, intrinsic carrier mobility, good chemical stability, and compatibility with wide-area printing, carbon nanotubes (CNTs) have been used for thin-film transistors using non-contact printing, primarily as a p-type semiconductor. The clear motivation for flexible CNT devices has driven research for >15 years,[155–157] leading to a relatively mature technology currently that is pushing into new areas in research labs. There are several strategies for developing printed CNT devices, which due to their high aspect ratio, and the desire to have long nanotubes for improved properties, can pose a challenge for reliable deposition. Common strategies involve inks containing semiconducting CNTs based on water/surfactant mixtures, select polar organic solvents, or stabilizing conjugated polymers in hydrocarbon solvents.[158–162] A key challenge for transitioning CNT-based devices is reliability and control over the interplay between CNT purity, size, concentration, printing characteristics, density and morphology on the surface, and device functionality. While several groups have effectively calibrated the process to balance device mobility (favored by higher density of CNTs) and on/off ratio (favored by lower density, high purity), generalizing this and controlling it well in a production setting requires clear focus.[158]

Metal oxide semiconductors gained popularity for display applications, offering a transparent semiconductor if oxygen vacancies can be well controlled in derivatives of zinc, tin, and indium oxides. Sol-gel approaches for deposition of these materials are a frequent strategy, with similar thermal limitations as described for metal oxide dielectrics. However, when the process temperature can be reduced or accommodated, these materials can offer competitive mobility to organic materials and sufficient performance for a range of device applications. Because their electronic properties are driven by oxygen vacancies, effectively controlling vacancy concentration via composition and processing is key to achieving stable, high-performance devices. Indium-gallium-zinc oxide (IGZO) is one example in this category which is suited for transistors. This n-type semiconductor gained prominence in display technologies due to high carrier mobility characteristics, reduced leakage current, and good optical transparency. Due to its ternary nature, the composition can be

varied to tailor the overall characteristics of printed devices.[163] The fabrication of IGZO channels for thin film transistors via inkjet printing has been realized in a wide range of literature reports.[164–166] As with CNT devices, this is reasonably mature within the research community,[167] and more recent efforts have extended these materials to broader application domains such as sensors, memory, and neuromorphic computing.[168–170]

While the optical transparency of metal oxide semiconductors motivates their use in transparent electronics, in the context of photovoltaics and optical sensing alternative materials are desired. Chalcogenides and perovskites are particularly suited for optoelectronic applications and have demonstrated compatibility with non-contact printing methods. Cu_2ZnSnS_4, for example, is an effective absorber for printed thin film solar cells. In the case of perovskites, devices fabricated via aerosol jet printing have been demonstrated for detection of x-rays.[171,172] In both cases, it is generally more common to print precursor or molecular inks, which are converted to the semiconductor composition and crystallinity following printing and post-processing. Certain chalcogenide materials can also be leveraged for their thermoelectric properties. Ag_2Se, for example, has good thermoelectric properties even at modest temperatures. It was adopted for inkjet printing via the dispersion of Ag_2Se nanoparticles in ethanol followed by sonication to obtain stable inks.[173] Others such as Sb_2Te_3 and $Bi_2Te_{2.7}Se_{0.3}$ have also been patterned on various substrates via aerosol jet printing to demonstrate thermoelectric devices with good power factor.[174,175]

In addition to these bulk semiconductors, there have been many efforts to develop semiconducting 2D materials for printable inks.[176] Because this is thoroughly discussed in more focused literature reviews elsewhere,[177,178] we forego repetition here. In general, this class of materials offers diverse functionality with inherent characteristics for liquid-phase processing. Due to the polydisperse nature of flakes, extra effort is demanded to control flake geometry, as it impacts both printing characteristics and device functionality.

There is clear potential for printed devices of various functionalities to be realized with semiconducting inks, making them a continued focus area for research efforts. However, the diverse fragmentation of applications, and thus key metrics, makes it challenging to develop meaningful figures of merits that generalize between use contexts, and complicates the business case for transitioning successful laboratory demonstrations of materials beyond research labs.

3.4. Ink formulation

While the discussion here is focused primarily on the functional materials, the broader ink formulation is of course critical for realizing the greatest potential for a given material. While the combination of dispersants, additives, and solvents that makes an ink an ink rarely increases the performance potential of a given material beyond its intrinsic properties, it can certainly result in inferior manufacturability and functionality if not given proper attention. Some ink formulation criteria are fairly explicit, such as achieving viscosity within the suitable range for a printing system. Others are more nebulous, such as understanding how the rheology evolves as the printed material dries, or understanding coupling between the ink composition and processing parameters. Given the complexity and practical relevance of this topic, there is extensive literature on printability that in many cases has not been fully extended to functional nanomaterial inks.[179]

In many laboratory efforts, crude formulation of inks centers on solvent selection and composition. Blends of solvents frequently provide greater flexibility to tailor chemical, fluid, and transport characteristics of inks compared to single-solvent compositions. While typical commercial inks contain complex combinations of solvents, cosolvents, and additives, many laboratory-developed formulations rely on only one or two solvents. This is often practical for demonstration and material evaluation, but more sophisticated formulations are expected to be useful to improve printability and tailor characteristics for manufacturing-centric metrics. Explicit standards driven by manufacturing process compatibility and maturity, rather than material functionality for a one-off laboratory demonstration, could more broadly accelerate advances in printability that consider stability and variability relevant to a production environment.

4. Post Processing

4.1. Role and considerations

Most inks require some form of post processing step to convert the deposited 'green' material to a functional, typically solid, material. This can be as simple as drying, but more often involves sintering for metallic materials,[180] or curing for some polymers.[181] This step plays a key role in the process flow for printed electronic devices, and materials compatibility in the context of post processing can impose strict constraints on materials selection and process design.[182] While there are different methods for effecting this transformation, and the transformation itself can be chemical, physical, or a combination, it almost always requires the input of energy into the printed material, and can alter the microstructural, electrical, and mechanical properties of printed materials (**Figure 4**).[183,184] As a typical example, a silver nanoparticle ink might contain ligands, dispersants, and high boiling solvents to support ink stability and compatibility with the printing method.[185] During a thermal sintering step, remaining solvents would be evaporated, and ligands and dispersants could be burned off or degraded enough to volatilize. In addition, the silver nanoparticles would sinter together to improve electrical conduction pathways between adjacent particles, reduce porosity, and improve mechanical cohesion. For many polymer dielectric inks, curing via application of UV light will chemically polymerize photoactive monomers to convert a liquid resin into a solid polymer film, and thermal curing is also applicable to thermoset materials. The type of post processing treatment is thus highly dependent on the materials chemistry, but for some materials, such as conductive inks, there exist several options that can be assessed based on time, compatibility with substrates and other materials, reliability, and equipment cost.

View Article Online
DOI: 10.1039/D5NR02110C

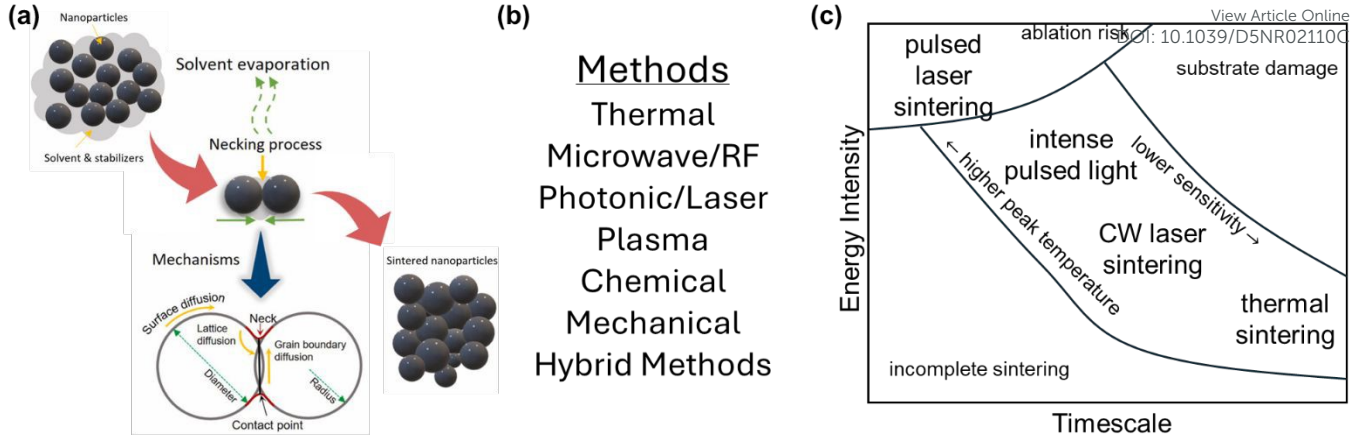

Figure 4. Post processing approaches for nanomaterial inks. (a) Illustration of drying and sintering mechanisms for nanoparticle-based inks; adapted with permission from Ref 194 (CC BY). (b) Classification of various methods to achieve sintering or annealing in printed materials. (c) Example of energy-time map for thermal and pseudo-thermal post-processing techniques.

4.2. Thermal sintering

Thermal sintering is simple and accessible, and has proven to be effective, so it serves as a reasonable benchmark. For a standard silver nanoparticle ink, it might be performed at moderate temperature (100 – 300 °C) in an oven or a furnace. Hotplates are also commonly used, particularly in laboratory environments, but may lead to uneven heat treatment within the print, uncontrolled convective environment around the sample, and a less direct route to implementation in typical fabrication lines. Thermal sintering commonly requires careful control of the temperature and time, along with ramp profile, for effective sintering without substrate damage or excessive energy and time. The sintering requirement is a strong driver for materials development, motivating inks that exhibit lower processing temperatures (70 – 90 °C) to broaden compatibility with temperature-sensitive substrates.[186–189] Despite its apparent simplicity, even thermal sintering approaches can be sensitive to details of the thermal environment and gradients, with some materials responding differently to drying/sintering sequence and heating from the substrate compared to the free surface of the ink.[190] As a result, even this fairly basic element of post-processing would benefit from more systematic analysis and theoretical understanding.

4.3. Alternatives

Given the time and energy requirements of thermal post processing, alternative methods have been under investigation for some time. Many of these rely on coupling energy directly into the printed material using electromagnetic radiation, whether in the form of radio frequency waves, broadband light, or laser light. An illustrative example is intense pulsed light (IPL) sintering,[184] which delivers short duration (~ms) pulses from a broadband light source. By locally heating the conductive ink due to its high absorptivity, and keeping the pulse duration short, high temperatures can be achieved within the printed material to effect very rapid sintering or curing with minimal thermal load to the substrate. It can be used for roll-to-roll processes and thus reduce cost and complexity. Laser sintering operates under a similar mechanism, albeit typically different power and timescale. Selective laser sintering has been found to rapidly sinter at temperatures up to 500 °C, which can cause rough surfaces to form and damage substrates in the case of polymers or other heat sensitive substrates. While slower than IPL, the spatial specificity of laser sintering can be particularly useful when there are multiple materials integrated on a surface and heating needs to be localized.[191,192]

A second broad alternative to thermal curing is chemical sintering. This allows for room temperature sintering of printed conductive traces. With ink chemistry tailored to this, one demonstration of this leverages exposure to an acidic vapor environment,[83] which in this case caused desorption of additives and subsequent particle fusion. This method is particularly beneficial for temperature sensitive substrates, but can complicate processing, particularly if multiple materials are printed. Another approach involves printing the acidic solution onto the conductive trace and subsequently drying any solvent at low temperature.[83] Plasma sintering has also been studied, as it enables lower temperatures and reduced time to be used in the process of sintering due to the chemical activation of surfaces from the plasma.[191] Low temperature nonthermal plasma sintering is an alternative to standard plasma sintering as it mitigates thermal effects on delicate and flexible substrates.[193] One motivation for plasma sintering is the ability to leverage chemical activation while retaining reasonable suitability for scalable processing. Figure 4 illustrates broad methods used to post-process printed electronic devices in literature.[194] Several more recent approaches to enhance nanoparticle sintering include induction heating, electrical sintering, damp heating sintering, and near-IR sintering to reduce processing time, limit substrate heat exposure, and improve material properties.[195–198]

5. Application Demonstration

5.1. Passive electronics

View Article Online
DOI: 10.1039/D5NR01410C

The ability to print passive components, such as resistors, capacitors, and inductors, generally requires a step up in complexity from basic material and print evaluation. The possibility of augmenting the manufacture of printed circuit boards with fully printed passive components could offer size and weight advantages while supporting greater flexibility and form factor versatility than traditional discrete components. In many cases, these passive components require integration of multiple materials, often in multilayer structures, and thus demand material and process compatibility along with reasonable registration and alignment. Demonstrations have been done with different print technologies (**Figure 5**a), including notable efforts to target specific electrical characteristics.[199–201] Precision and reproducibility of these printing methods remains a challenge even for relatively basic electronic devices, but in many cases these engineering and manufacturing aspects elude the focus of research laboratories.

Of course, the ability to recreate functionality of basic circuit elements, which are widely available as standardized surface mount components at low cost and high reliability, is a necessary effort but not the ultimate objective. Improving on the functionality of these – for example, by supporting flexible or stretchable designs or accommodating operation in extreme environments – would provide a greater value proposition for these printing technologies.

In many cases, capacitance achieved in printed devices is limited by inherent challenges in coupling a thin dielectric layer with multilayer structures. Manufacturing process reliability and pinhole prevention make this a challenge even for basic metal-insulator-metal capacitors, with yield challenges if these are stacked to increase capacitance in a given footprint of the substrate. Inductors, on the other hand, often support limited current flow owing to the coil length and the generally thin nature of printed conductors in comparison to electrolytic copper. In contrast to planar inductors, Gu, et al. demonstrated relevant inductance values for solenoid-type devices using polymer, iron, and ferrite cores, leveraging the conformal patterning capability of aerosol jet printing.[202]

5.2. RF electronics

Another area in which the design flexibility of printed components, and direct integration onto the substrate, offers promise is extending from low frequency to radio frequency (RF) circuits. In this regard, printing technologies have been employed to fabricate custom transmission lines and other passive components for operation at GHz frequencies.[203–205]

Antennas provide another case for which the large-area patterning, conformal printing, and rapid prototyping capabilities of non-contact printing methods carry significant advantages (Figure 5b). A wide range of antennas have been demonstrated,[206–208] including conformal devices and complex antenna arrays with completely printed building blocks.[209] In addition, complex metasurface antenna designs exemplify the design flexibility of these printing methods, and highlight the complex interplay of device design and fabrication required for multi-axis printing.[210] One challenge less apparent under low frequency conditions is the sensitivity to porosity, roughness, and defects. The issue of surface roughness and material quality associated with prints should therefore be more thoroughly addressed to reduce losses of these high frequency devices and allow them compete with conventional technologies.[211,212]

5.3. Hybrid electronics

Substantial early efforts in printed electronics focused on active devices such as transistors, and this capability continues to have significant potential. However, hybrid electronics that combine printed components with conventional microelectronics are increasingly attractive for a broad range of practical implementations (**Figure 6**).[20,213,214] This paradigm allows complementary use of reliable, low-cost, and high-performance microelectronics with large-area, flexible, stretchable, and conformal printed elements. Here, these printing technologies often have access to a broader range of materials than conventional microfabrication, including biomaterials and nanomaterials. Moreover, the material sets accessible to printing methods can be tailored to unique environmental conditions, such as high temperatures or stretchability requirements, which are not well served by traditional, large-scale electronics fabrication.

In this context, a key technical challenge is designing and controlling the interface between printed and microfabricated components.[215,216] Printed conductors on polymer substrates often have poor compatibility with conventional solders,[217,218] motivating strategies for printed interconnects.[219] This is a

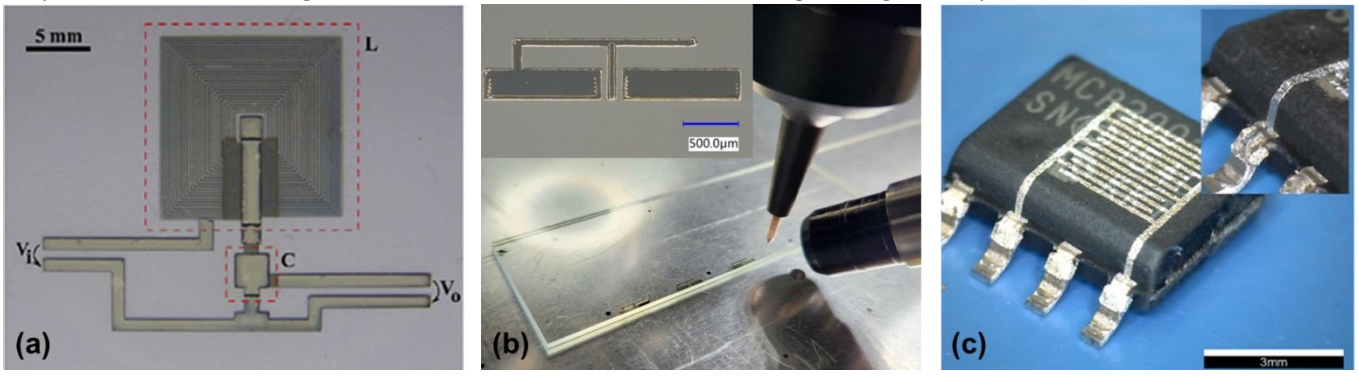

Figure 5. Demonstrator applications for droplet-based printed electronics. (a) Low-pass filter with capacitor and inductor elements. (b) Passive components for high frequency electronics, including transmission lines and radial stubs. (c) Humidity sensor printed directly onto a packaged integrated circuit. Graphics adapted with permission from Ref. 201, 208 (CC BY), and 230 (CC BY), respectively.

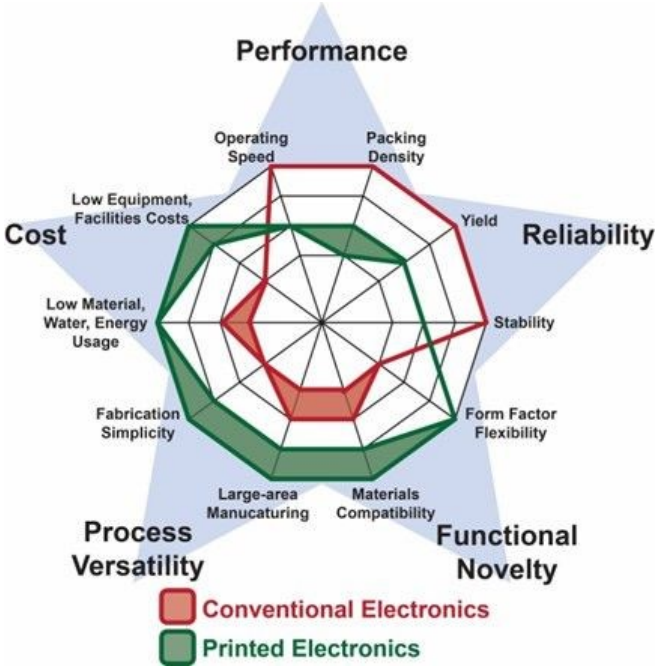

Figure 6. Rationale for hybrid circuits combining conventional and printed technologies; reprinted with permission from Ref. 121.

compelling area for research, and provides a practical route to integrate printed materials and components into more complex systems. Extending this approach to photonic devices, as highlighted by printed waveguide structures, provides another promising area of research for practical applications.[220–222]

5.4. Sensing

Sensors represent a prominent, and broad, application area for printed devices, as they leverage the material and design versatility of non-contact, digital fabrication technologies. Among many application prototypes, sensors have been demonstrated for chemical stimuli such as pH,[223] gases,[224] and biochemicals,[225] along with physical and electromagnetic stimuli such as temperature,[226] deformation,[227] light,[228] and capacitance.[229] Integration with flexible, stretchable, and conformal surfaces amplifies the opportunities for implementing printed sensors in a wide variety of applications (Figure 5c).[230]

Effectively comparing the performance of sensors made by individual printing methods is difficult due to the widely varying characteristics of interest and metrics adopted for performance evaluation. Stability and reliability of printed sensors, which encompasses manufacturing process reproducibility, is of particular importance for maturing printed sensors to address the broad range of applications where they offer meaningful benefits. While many research efforts demonstrate individual sensors for specific stimuli, multiplexed sensors that can compensate for interference, allow spatial specificity, or increase the range of chemical analytes will continue to increase in sophistication. Machine learning methodologies to deconvolute, simplify, and interpret large amounts of data from printed sensors will be an important complement to the diversity of materials and device configurations.[231]

6. Outlook/Perspective

6.1. Digital integration

Recent years have witnessed a significant increase in efforts to implement machine learning and advanced data analytics into the process flow for printed electronics research, owing in large part to expansion in computational power and democratization of machine learning capabilities.[232] In most cases, this research has focused on automating and improving process development in the area of print parameter optimization. Each printing method is defined by a wide phase space of controllable parameters that interact with specific physics of the ink in complex ways. Optimization of these parameters is often largely manual, based heavily on qualitative observations and prior experience, and incomplete. There are therefore considerable advantages to be gained in standardization, efficiency, and quality by incorporating state-of-the-art data analytics methodologies for these tasks.

We summarize a subset of these efforts in **Table 2**. For AJP, this research commonly leverages image analysis to classify line quality, with several works including functional properties such as resistance. For the most part, these efforts vary the digitally controlled printing parameters, such as gas flow rates and print speed, and have not yet extended to 'low frequency' variables such as ink composition and nozzle size. For IJP, there have been several interesting studies applying image analysis and high throughput experimentation to the droplet generation process itself, tailoring the waveform for droplet ejection, which can include predicting droplet velocity and size based on the ink properties. In addition, imaging following deposition can be applied as a predictor of print quality. A similar approach can be leveraged for EHD printing,[233] using imaging of the printer nozzle to classify the jet characteristics. In addition, as for AJP, print parameters such as flow rate, speed, and voltage can be connected to both geometric metrics of print quality and electrical characteristics.

These applications of machine learning serve a dual purpose. When narrowly applied, for example to a particular ink, they provide a methodology to accelerate process optimization. More broadly, when machine learning is used to tease out connections between ink properties, print parameters, and process outcomes, this can reflect insight on the physical mechanisms of the process. This second approach, while more ambitious and complex, has strong potential to complement traditional methods, but this is somewhat contingent on the transparency or interpretability of the machine learning models.

Optimization of machine parameters for printing is a fairly well-defined and compartmentalized problem that lends itself well to rapid iteration to build up datasets with full digital control. A noteworthy example from the space of direct ink writing, by Deneault, et al., developed an autonomous research system with Bayesian optimization (**Figure 7**a).[234] It is thus reasonable that this constitutes an initial major foray of machine learning into additive electronics, but it is not the complete picture. In particular, while iteration over process parameters can be performed digitally in a purpose-built

fabrication system, iteration over materials or ink formulations largely remains manual and thus relatively slow. While this is thus a less realistic target for short-term research advances in efforts limited to an individual lab or small research team, the complexity of ink formulation and non-continuous nature of many variables makes it a compelling target for future research where the scale and capability of sophisticated data analytics tools offer meaningful benefits. In this context, more standardized approaches to ink evaluation – even without the context of machine learning – would be valuable to establish broad datasets that allow meaningful comparison. Moreover, framing the test methodology on foundational process physics could support more efficient development and generalization than purely empirical approaches.

Table 2. Sampling of machine learning demonstrations applied to digital printing

Target output	Model input	ML Methods	Ref.
Inkjet Printing			
Drop size, velocity, formation	Voltage Frequency	Back propagation neural network	235
Drop velocity, formation	Waveform Ink properties	MP	236
Drop size, velocity, formation	Waveform Ink properties Nozzle size	Ensembles: DT, GB, RF	237
Line quality Electrical conductance	Environment Drop metrics Frequency	Convolutional neural net	238
Aerosol Jet Printing			
Line quality (edge)	Gas flow rates Print speed	Hybrid: SV, K-means	239
Electrical resistance	Gas flow rates Print speed	Sparse rep. classification	240
Line thickness Line width	Gas flow rates Print speed	Hybrid: SV, GP	241
Electrical resistance	Gas flow rates Print speed	Hybrid: MP, RL	242
EHD Jet Printing			
Electrical conductivity	Print speed Ink flow rate Voltage	RF K-NN	243
Droplet diameter	Ink properties Nozzle size, standoff, flow rate, voltage	Artificial Neural Network	244
Droplet diameter Ejection frequency	Ink properties Pulse settings Flow rate Nozzle size, standoff	Various; GB regression best	245
Line width	Settings (standoff, voltage, speed) In-situ images	Ensemble	246

Acronym legend – RF: random forest; GB: gradient boosting; DT: decision tree; MP: multilayer perceptron; K-NN: k-nearest neighbors; SV: support vector; GP: Gaussian process; RL: reinforcement learning

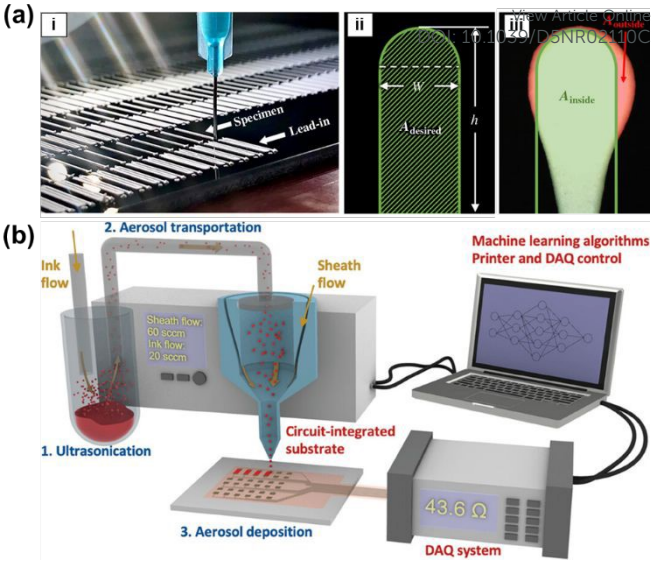

Figure 7. Application of advanced computational methods for digital printing. (a) Example of autonomous research system for closed-loop optimization of direct ink writing, in which computer vision feedback is combined with Bayesian optimization and printer control to optimize print parameters; adapted with permission from Ref 234 (CC BY). (b) Hybrid machine learning approach for AJP, which allows direct optimization on the functional characteristics of the printed materials, in this case resistance measurements; adapted with permission from Ref 242.

A more approachable near-term target may be multi-objective optimization with constraints on training data size. Additive electronics is not naturally a big data problem, at least if the focus is on process optimization for a single ink. The work of Du, et al. is a clarifying example to illustrate this,[242] focusing on iterative optimization with minimal data, and including both geometric and functional properties (Figure 7b).

Notably, this is a dynamic research area with broad interest, and will continue to evolve rapidly in coming years.[247] Increasingly sophisticated methods incorporate multimodal data streams and multiobjective optimization across scales. Furthermore, machine learning toolsets are becoming more broadly accessible, allowing a wider range of practitioners with interests across materials, methods, and applications to leverage these capabilities. While many of the early demonstrations zero in on process parameter optimization, broader application in part design for additive manufacturing,[248] along with digital twins for defect prediction or real-time adaptive control,[249,250] provide just some examples of the compelling opportunities in this space to augment physics-based process understanding.

Going forward, it is instructive to observe the applications of machine learning in other research domains. In particular, there are broad and successful efforts to apply machine learning in the space of materials science, leveraging broad communities with common data standards. Merging materials and process optimization in a similar manner could have significant benefits for practitioners of printed electronics. Notably, several studies applying ML methods to printed electronics have sourced data from the literature,[237,245] hinting at the logical transition to larger data sets. This is challenged by limited standardization in data collection and reporting across research labs, but larger

efforts to address this could meaningfully change the scope with which artificial intelligence could be applied to augment material and process development.

Finally, there should also be fair consideration given to digital approaches to improve these processes that rely on more traditional and straightforward methods. Where robust theory and understanding exists, there is less need for opaque machine learning models. This is supported by various efforts to apply computational fluid dynamics for process modelling, along with deterministic and physics-based control approaches.[58,251–255] While complex, printed electronics is not nearly as much so as the stochastic and often chaotic phenomena for which big data methodologies excel, and physics-based understanding of processes can better support generalization, adaptation, and extrapolation to new systems.

6.2. Multimaterial patterning

An application area where the aerosol jet printing technology in principle excels is multimaterial device manufacturing. Specifically, multiple chemically distinct aerosol ink streams can be merged into a single jet, leading to the deposition of composite traces with tailorable composition and physical properties. This concept is adapted from DIW printing, for which numerous demonstrations have shown the utility of multimaterial printing, typically for larger scale parts.[256,257] In this configuration, two distinct kinds of devices can be printed, the first one being a composite structure with a spatially constant chemical composition intermediate from the two source inks or, alternatively, the relative deposition rate can be dynamically controlled during the manufacturing of a single component to fabricate thin film functionally graded materials (**Figure 8**a).

Early adopters of this peculiar manufacturing approach for AJP included Reitz, et al., for grading composition vertically in a solid oxide fuel cell stack,[258] along with Wang, et al. for varying electrical properties in CNT/polyimide nanocomposites.[259] More recently, Craton, et al. demonstrated RF components with the multimaterial aerosol jet printing technique.[260,261] In one instance, the authors demonstrated spatial tailoring of film dielectric constant by mixing a polyimide dielectric aerosol stream with one containing $BaTiO_3$, leading to a ~1.4 µm thick film with a dielectric constant between 3.1 and 8.9.[261] They leveraged the same technique to mix nickel-zinc-ferrite nanoparticles in a static ratio into a polyimide matrix, which resulted in a 40% increased inductance with respect to similar planar inductors.[260] A boost in recognition for this capability arose due to thorough work by Zhang, et al., with the broad demonstration of combinatorial printing using multimaterial AJP,[262] including demonstrations for both thermoelectrics and later solid state electrolytes for LIBs.[263] Gamba, et al. investigated multimaterial aerosol jet printing for the manufacturing of functionally graded materials. In one instance, the researchers mixed metallic aluminum nanoparticles with copper (II) oxide with constant stoichiometric ratio to fabricate high resolution nanothermites, which were later deposited on a silver resonator for wireless RF ignition.[264] This result was enabled by the unique setup of AJP, leading to high resolution single pass thermite lines while also preventing premature mixing and potential accidental ignition of the fuel, increasing operational safety. In the same study, functionally graded manufacturing was also demonstrated with the same inks. The effect of the printhead design was correlated to the microscopic morphology of the energetic composites and it was concluded that static mixing elements within the printhead significantly enhance material mixing in the final traces. In a separate work, Gamba, et al. tailored electrical properties of carbon nanomaterial traces by mixing graphene and carbon nano onions with different stoichiometries, printing composites with either fixed mixing ratio or a compositional gradient.[265] This

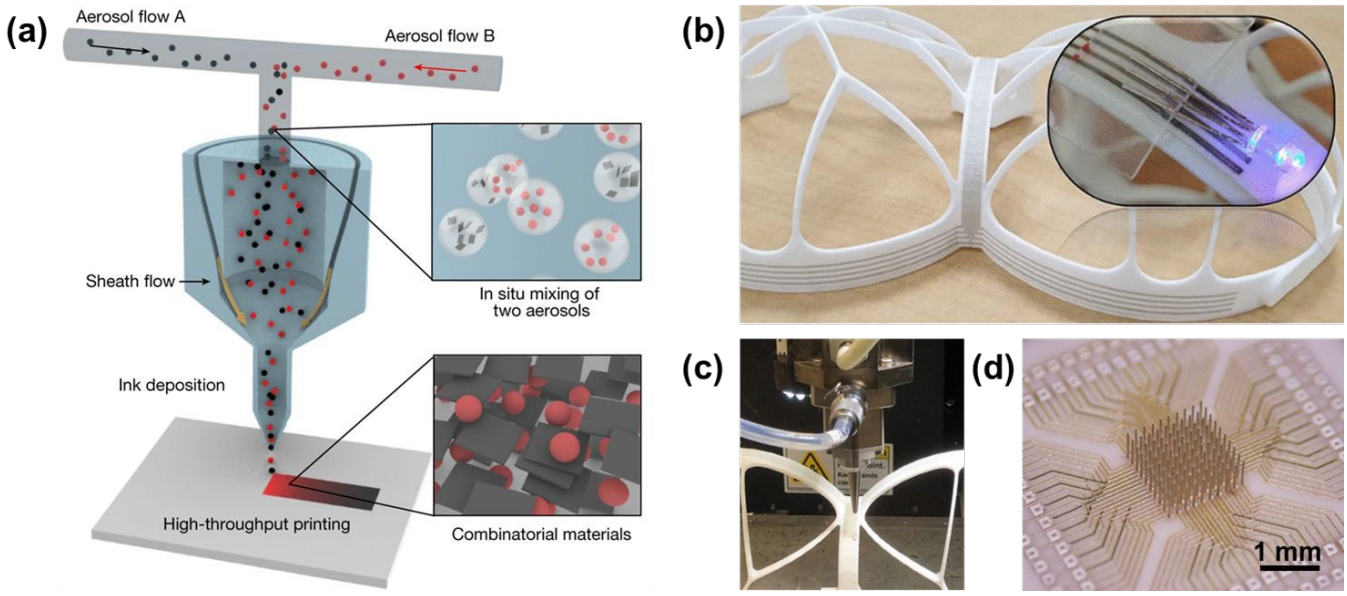

Figure 8. (a) Multimaterial aerosol jet printing, in which two ink streams are mixed in situ to create gradient patterns, in this case for combinatorial screening of materials. (b, c) Conformal printing of conductive traces onto a drone safety cage using AJP. (d) High aspect ratio microelectrode array printed with AJP. Graphics adapted with permission from Ref. 262 (CC BY), 268, and 189 (CC BY-NC), respectively.

View Article Online
DOI: 10.1039/D5NR02110C

allowed patterning of functional materials with electrical resistivity spanning two orders of magnitude, which could allow resistance targeting over a broad range by tailoring both the physical geometry of a part and its composition and intrinsic properties.

A compelling application of gradient printing was recently demonstrated by Zhang, et al.[266] In this work, the authors prepared a mechanically graded interface by combining polyurethane dispersions with distinct stiffness. This allowed the graded substrate to interface well with skin via a soft polyurethane, with a smooth gradation to a harder surface to support electronics. This configuration allowed high performance electronics integrated on skin with considerable strain insensitivity, and broadly highlights the utility of multimaterial printing for creating controlled, diffuse interfaces.

6.3. Beyond thin film printed electronics

Recent years have witnessed droplet-based printing methods evolving to more challenging environments and architectures beyond planar, thin-film printed electronics.[262,267,268] In the context of these methods, 3D printing can be a nebulous label with varying usages. We will briefly describe several flavors of this terminology, broadly classified as multilayer, conformal, high aspect ratio, and freeform 3D printing.

Multilayer electronic circuits are highly sought for functional devices, and in many cases parallel the architectures of more traditional built-up substrates used in electronics packaging. In these most common instantiations, multilayer electronics at their simplest require deposition of both conductive and dielectric materials, with the compatibility between inks a critical determinant of functionality. This encompasses both materials compatibility in the final part (e.g., adhesion, interfacial strength) and considerations of process compatibility (e.g., curing conditions, solvent orthogonality). Several commercial suppliers have moved into this space, with Nano Dimension an early entrant using inkjet technology. The value of these platforms remains highly dependent on material properties, with dielectric materials often imposing limitations in thermal, mechanical, or electrical performance. Among the three droplet-based printing methods discussed here, inkjet has seen the most maturation towards multilayer circuits, largely a result of its scaling advantages due to parallel jetting, and direct ink writing approaches offer a useful guide, albeit typically for circuits with coarser resolution.[269–272] At a high level, droplet-based printing methods with digital control have a potential advantage for such multilayer circuits. In particular, the digital control offers a possibility to adjust the print pattern to compensate for variations in previous fabrication steps, a part-by-part versatility that is not matched by methods with hard tooling. However, the realization of this remains largely limited to very narrow, proof of concept demonstrations. One advantage that noncontact, direct write printing offers for multilayer circuitry is the ability to localize insulating material to crossovers and other key places, reducing the overall amount of material and weight of the part compared to a traditional printed circuit board. Extending this concept to optical materials with multimaterial inkjet printing, researchers have developed gradient index lenses and sophisticated optics that hint at the scope of applications beyond electronics.[273]

The second flavor of 3D patterning for droplet-based methods is conformal printing, which describes the fabrication of thin film electronics on curved, 3D surfaces (Figure 8b-c). This is a compelling application space not well served by master-based printing methods or most traditional fabrication technologies, offering a clear value proposition for digital printing. Conformal integration of electronics directly on structural components offers form factor flexibility with associated space and weight savings. This is particularly relevant to support miniaturization in high-value constrained applications, such as wearable devices, aerospace and automotive systems, biomedical devices, and space electronics.[274] Moreover, direct integration of components such as sensors without an intermediating substrate can provide closer contact with structures for more precise sensing, for example in the case of thermal sensing and structural health monitoring.[275] Nonplanar geometries can furthermore offer unique functionality for optics applications,[276] along with versatility for hybrid augmentation of populated circuit boards or in-place repair.[277] Among the methods discussed here, AJP is a highly compelling technology for conformal printing, with a high velocity jet that can maintain fine resolution even up to standoff distances of 5 mm.[278] This offers key tolerance for contouring complex surfaces. Moreover, the suitability of AJP for deposition in an oblique configuration, which is supported by partial drying and resulting rheology changes prior to droplets hitting the surface, gives additional versatility for motion planning.[279] Some prominent examples of conformal electronics include sensing systems,[17,268] biomedical devices,[280] antennas,[281] and microinductors.[282]

The last two, related flavors of microscale 3D printing discussed here are patterning for high aspect ratio (height: width) features and spanning structures in more complex configurations. AJP is again a promising technology for the demonstration of these capabilities, owing in part to its high standoff capability and suitability for printing high viscosity materials. In the area of printing high aspect ratio structures, Panat, et al. have demonstrated compelling applications of microelectrode arrays for biological sensing (Figure 8d).[27,267] The same group pioneered AJP for spanning 3D structures that qualify as freeform 3D printing, showcasing complex lattice structures and their application as current collectors for batteries.[27,283] In all these cases, self-supporting structures are enabled by printing materials that rapidly solidify following deposition, largely through the traditional means of solvent evaporation.[284] In a different approach, Akyurtlu, et al. demonstrated patterning of a dielectric polymer by rapid UV curing to create sophisticated 3D structures,[285] with the 100% solids loading ink supporting relatively rapid fabrication. EHD jet printing also offers interesting alignment for certain high aspect ratio structures, such as micropillars.[286] In this context, the shape of the electric field around previously-deposited material

View Article Online
DOI: 10.1039/D5NR02110G

can enable precise structures approaching micron-scale diameter.[287]

7. Conclusions

Digital, high resolution material jetting technologies have exhibited considerable growth, and are accelerating into more sophisticated and varied application spaces as the ecosystem across materials, digital capabilities, and applications matures. Inkjet, EHD, and aerosol jet printing offer versatile technologies for integrating functional materials in complex configurations. A holistic view, spanning the fundamental process physics, ink formulation, printing, and post processing is necessary to best leverage these technologies in emerging applications, and can provide a versatile foundation to rationally apply data-driven methods. As this technological field advances, research efforts generally shift from core materials and capability development to applied topics. However, there is a continued need for generalizable, fundamental understanding as it relates to ink formulation, material integration, and post-processing, and a coherent bridge between these scientific studies and engineering tools will accelerate adoption and adaptation. The fragmented nature of the commercial landscape for digital printed electronics provides limited incentive thus far to coalesce around materials or fabrication technologies, suggesting that this field largely remains in a phase of exploration that can yield rapid, unexpected advances but without a strong, single application pull that would shape the technologies for commercial use and enforce greater standardization, cooperative roadmaps, and an emphasis on cost and reliability. Organizations aiming to add this higher-level ecosystem maturity thus have a clear challenge, and will play an important role in shaping the field's evolution. This creates a rich and dynamic research environment, but also necessarily tempers expectations for near-term commercial successes and analogies to incumbent electronics technologies. Meanwhile, continued advances in materials, process understanding, digital controls, and creative device design promise exciting advances in these technologies in coming years and their further maturation to enable the broader vision of printed and hybrid electronics and extend these toolsets for applications beyond electronics.

Author contributions

E.B. Secor: Writing – Original Draft (lead), Conceptualization (lead); **D. Yeboah:** Writing – Original Draft (support); **L. Gamba:** Writing – Original Draft (support).

Conflicts of interest

There are no conflicts to declare.

Data availability

No primary research results, software or code have been included and no new data were generated or analysed as part of this review.

Acknowledgements

The authors acknowledge support from the National Science Foundation under CMMI-2336356.

References

1 W. Wu, *Nanoscale*, 2017, **9**, 7342–7372.
2 A. Kamyshny and S. Magdassi, *Small*, 2014, **10**, 3515–3535.
3 L. Nayak, S. Mohanty, S. K. Nayak and A. Ramadoss, *J. Mater. Chem. C*, 2019, **7**, 8771–8795.
4 J. Q. Feng and M. J. Renn, *J. Micro Nano-Manuf.*, 2019, **7**, 011004.
5 M. S. Onses, E. Sutanto, P. M. Ferreira, A. G. Alleyne and J. A. Rogers, *Small*, 2015, **11**, 4237–4266.
6 A. C. Arias, J. Daniel, B. Krusor, S. Ready, V. Sholin and R. Street, *J. Soc. Inf. Disp.*, 2007, **15**, 485–490.
7 Y. Zheng, Z. He, Y. Gao and J. Liu, *Sci. Rep.*, 2013, **3**, 1786.
8 S. Stoukatch, P. Laurent, S. Dricot, F. Axisa, L. Seronveaux, D. Vandormael, E. Beeckman, B. Heusdens and J. Destiné, in *2012 4th Electronic System-Integration Technology Conference*, 2012, pp. 1–5.
9 H. R. Khaleel, *IEEE Trans. Compon. Packag. Manuf. Technol.*, 2014, **4**, 1722–1728.
10 A. Mette, P. L. Richter, M. Hörteis and S. W. Glunz, *Prog. Photovolt. Res. Appl.*, 2007, **15**, 621–627.
11 H. Abdolmaleki, P. Kidmose and S. Agarwala, *Adv. Mater.*, 2021, **33**, 2006792.
12 V. K. R. R., V. A. K., K. P. S. and S. P. Singh, *RSC Adv.*, 2015, **5**, 77760–77790.
13 J. Li, F. Rossignol and J. Macdonald, *Lab. Chip*, 2015, **15**, 2538–2558.
14 E. Jabari, F. Ahmed, F. Liravi, E. B. Secor, L. Lin and E. Toyserkani, *2D Mater.*, 2019, **6**, 042004.
15 M. Smith, Y. S. Choi, C. Boughey and S. Kar-Narayan, *Flex. Print. Electron.*, 2017, **2**, 015004.
16 J. U. Park, M. Hardy, S. J. Kang, K. Barton, K. Adair, D. K. Mukhopadhyay, C. Y. Lee, M. S. Strano, A. G. Alleyne, J. G. Georgiadis, P. M. Ferreira and J. A. Rogers, *Nat. Mater.*, 2007, **6**, 782–789.
17 J. A. Paulsen, M. Renn, K. Christenson and R. Plourde, in *2012 Future of Instrumentation International Workshop (FIIW) Proceedings*, 2012, pp. 1–4.
18 Y. Huang, H. Wu, L. Xiao, Y. Duan, H. Zhu, J. Bian, D. Ye and Z. Yin, *Mater. Horiz.*, 2019, **6**, 642–683.
19 J. Zikulnig, S. Chang, J. Bito, L. Rauter, A. Roshanghias, S. Carrara and J. Kosel, *Adv. Sens. Res.*, 2023, **2**, 2200073.
20 Y. Khan, A. Thielens, S. Muin, J. Ting, C. Baumbauer and A. C. Arias, *Adv. Mater.*, 2020, **32**, 1905279.
21 Y. Gu, D. R. Hines, V. Yun, M. Antoniak and S. Das, *Adv. Mater. Technol.*, 2017, **2**, 1700178.
22 A. Sherehiy, D. Jackson, M. Sassa, D. Sills, D. Ratnayake, R. Zhang, Z. Yang, K. Walsh, J. Naber and D. O. Popa, *J. Micro Nano Sci. Eng.*, 2025, **13**, 011003.
23 M. T. Craton, X. Konstantinou, J. D. Albrecht, P. Chahal and J. Papapolymerou, *IEEE Trans. Microw. Theory Tech.*, 2020, **68**, 3418–3427.

24 S. Lu and A. D. Franklin, *Nanoscale*, 2020, **12**, 23371–23390.
25 R. Sliz, M. Lejay, J. Z. Fan, M.-J. Choi, S. Kinge, S. Hoogland, T. Fabritius, F. P. García de Arquer and E. H. Sargent, *ACS Nano*, 2019, **13**, 11988–11995.
26 K. Parate, S. V. Rangnekar, D. Jing, D. L. Mendivelso-Perez, S. Ding, E. B. Secor, E. A. Smith, J. M. Hostetter, M. C. Hersam and J. C. Claussen, *ACS Appl. Mater. Interfaces*, 2020, **12**, 8592–8603.
27 Md. A. Ali, C. Hu, S. Jahan, B. Yuan, M. S. Saleh, E. Ju, S.-J. Gao and R. Panat, *Adv. Mater.*, 2021, **33**, 2006647.
28 Y. Saitoh, K. Sumiyoshi, M. Okada, T. Horii, T. Miyazaki, H. Shiomi, M. Ueno, K. Katayama, M. Kiyama and T. Nakamura, *Appl. Phys. Express*, 2010, **3**, 81001.
29 J. Daniel, A. C. Arias, W. Wong, R. Lujan, S. Ready, B. Krusor and R. Street, *Jpn. J. Appl. Phys.*, 2007, **46**, 1363.
30 K. Cao, Y. Liu, G. Meng and Q. Sun, *IEEE Access*, 2020, **8**, 85714–85728.
31 M. Zeng and Y. Zhang, *J. Mater. Chem. A*, 2019, **7**, 23301–23336.
32 X. Zeng, P. He, M. Hu, W. Zhao, H. Chen, L. Liu, J. Sun and J. Yang, *Nanoscale*, 2022, **14**, 16003–16032.
33 J. Li, W. Tang, Q. Wang, W. Sun, Q. Zhang, X. Guo, X. Wang and F. Yan, *Mater. Sci. Eng. R Rep.*, 2018, **127**, 1–36.
34 S. K. Garlapati, M. Divya, B. Breitung, R. Kruk, H. Hahn and S. Dasgupta, *Adv. Mater.*, 2018, **30**, 1707600.
35 Rahito, D. A. Wahab and A. H. Azman, *Processes*, 2019, **7**, 802.
36 G. L. Goh, H. Zhang, T. H. Chong and W. Y. Yeong, *Adv. Electron. Mater.*, 2021, **7**, 2100445.
37 H. Wu, Y. Tian, H. Luo, H. Zhu, Y. Duan and Y. Huang, *Adv. Mater. Technol.*, 2020, **5**, 2000093.
38 Z. Hou, H. Lu, Y. Li, L. Yang and Y. Gao, *Front. Mater.*, 2021, **8**, 647229.
39 C. Kant, A. Shukla, S. K. M. McGregor, S.-C. Lo, E. B. Namdas and M. Katiyar, *Nat. Commun.*, 2023, **14**, 7220.
40 B. Derby, *Annu. Rev. Mater. Res.*, 2010, **40**, 395–414.
41 N. F. Morrison and O. G. Harlen, *Rheol. Acta*, 2010, **49**, 619–632.
42 J. Stringer and B. Derby, *Langmuir*, 2010, **26**, 10365–10372.
43 P. He and B. Derby, *Adv. Mater. Interfaces*, 2017, **4**, 1700944.
44 D. Soltman and V. Subramanian, *Langmuir*, 2008, **24**, 2224–2231.
45 J. Park and J. Moon, *Langmuir*, 2006, **22**, 3506–3513.
46 S. Chung, M. A. Ul Karim, M. Spencer, H.-J. Kwon, C. P. Grigoropoulos, E. Alon and V. Subramanian, *Appl. Phys. Lett.*, 2014, **105**, 261901.
47 T. Kawase, H. Sirringhaus, R. H. Friend and T. Shimoda, *Adv. Mater.*, 2001, **13**, 1601–1605.
48 P. Naderi and G. Grau, *Flex. Print. Electron.*, 2024, **9**, 015001.
49 J. H. Cho, J. Lee, Y. Xia, B. Kim, Y. He, M. J. Renn, T. P. Lodge and C. Daniel Frisbie, *Nat. Mater.*, 2008, **7**, 900–906.
50 E. B. Secor, *Flex. Print. Electron.*, 2018, **3**, 35002.
51 P. Deepu, C. Peng and S. Moghaddam, *Exp. Therm. Fluid Sci.*, 2018, **92**, 243–247.
52 R. J. Lang, *J. Acoust. Soc. Am.*, 1962, **34**, 6–8.
53 R. R. Tafoya and E. B. Secor, *Flex. Print. Electron.*, 2020, **5**, 35004.
54 E. B. Secor, *Flex. Print. Electron.*, 2018, **3**, 35007.
55 B. I. Guyll, L. D. Petersen, C. L. Pint and E. B. Secor, *Adv. Funct. Mater.*, 2024, **34**, 2316426.
56 B. I. Guyll, B. L. Sanford, C. L. Pint and E. B. Secor, *Small Sci.*, 2025, **5**, 2500069.
57 G. Li, S. Wang, Z. Zhang, Y. Sun, J. Wen, J. Feng, S. Wang, Q. Sun and Y. Tian, *Adv. Mater. Technol.*, DOI:10.1002/admt.202402114.
58 S. Ramesh, C. Mahajan, S. Gerdes, A. Gaikwad, P. Rao, D. R. Cormier and I. V. Rivero, *Addit. Manuf.*, 2022, **59**, 103090.
59 USPTO, US12083548B2, 2024.
60 T. Ma, Y. Li, H. Cheng, Y. Niu, Z. Xiong, A. Li, X. Jiang, D. Park, K. Zhang and C. Yi, *Nat. Commun.*, 2024, **15**, 6317.
61 J.-U. Park, M. Hardy, S. J. Kang, K. Barton, K. Adair, D. kishore Mukhopadhyay, C. Y. Lee, M. S. Strano, A. G. Alleyne, J. G. Georgiadis, P. M. Ferreira and J. A. Rogers, *Nat. Mater.*, 2007, **6**, 782–789.
62 S. Mishra, K. L. Barton, A. G. Alleyne, P. M. Ferreira and J. A. Rogers, *J. Micromechanics Microengineering*, 2010, **20**, 095026.
63 B. H. Kim, M. S. Onses, J. B. Lim, S. Nam, N. Oh, H. Kim, K. J. Yu, J. W. Lee, J.-H. Kim, S.-K. Kang, C. H. Lee, J. Lee, J. H. Shin, N. H. Kim, C. Leal, M. Shim and J. A. Rogers, *Nano Lett.*, 2015, **15**, 969–973.
64 S. Mishra, K. L. Barton, A. G. Alleyne, P. M. Ferreira and J. A. Rogers, *J. Micromechanics Microengineering*, 2010, **20**, 95026.
65 C. Wei, H. Qin, N. A. Ramírez-Iglesias, C.-P. Chiu, Y. Lee and J. Dong, *J. Micromechanics Microengineering*, 2014, **24**, 45010.
66 S. An, M. W. Lee, N. Y. Kim, C. Lee, S. S. Al-Deyab, S. C. James and S. S. Yoon, *Appl. Phys. Lett.*, 2014, **105**, 214102.
67 S. Cai, Y. Sun, Z. Wang, W. Yang, X. Li and H. Yu, 2021, **10**, 1046–1078.
68 H. Yi, X. Guo, F. Chang, H. Cao, J. An and C. K. Chua, *Int. J. Extreme Manuf.*, 2025, **7**, 032002.
69 H. Li, Y. Li, G. Zhang, Y. Liu, Z. Han, H. Zhang, Q. Xu, J. Zhao, M. Jin, D. Song, M. Sun, F. Wang, X. Zhu and H. Lan, *Addit. Manuf.*, 2024, **96**, 104579.
70 Z. Li, W. He, Y. Zhang, J. Wang, G. Hu, Y. Wu and D. Li, *J. Manuf. Process.*, 2025, **133**, 1300–1309.
71 I. J. Fernandes, A. F. Aroche, A. Schuck, P. Lamberty, C. R. Peter, W. Hasenkamp and T. L. A. C. Rocha, *Sci. Rep.*, 2020, **10**, 1–11.
72 W. Yang, F. Mathies, E. L. Unger, F. Hermerschmidt and E. J. W. List-Kratochvil, *J. Mater. Chem. C*, 2020, **8**, 16443–16451.
73 N. Ibrahim, J. O. Akindoyo and M. Mariatti, *J. Sci. Adv. Mater. Devices*, 2022, **7**, 100395.
74 S. Magdassi, M. Grouchko, O. Berezin and A. Kamyshny, *ACS Nano*, 2010, **4**, 1943–1948.
75 M. Grouchko, A. Kamyshny, C. F. Mihailescu, D. F. Anghel and S. Magdassi, *ACS Nano*, 2011, **5**, 3354–3359.
76 P. Patil, S. Patil, P. Kate and A. A. Kulkarni, *Nanoscale Adv.*, 2021, **3**, 240–248.
77 Q. Zhang, D. Jiang, C. Xu, Y. Ge, X. Liu, Q. Wei, L. Huang, X. Ren, C. Wang and Y. Wang, *Sens. Actuators B Chem.*, 2020, **320**, 128325.
78 S. Lee, J. Jang, T. Park, Y. M. Park, J. S. Park, Y.-K. Kim, H.-K. Lee, E.-C. Jeon, D.-K. Lee, B. Ahn and C.-H. Chung, *ACS Appl. Mater. Interfaces*, 2020, **12**, 6169–6175.
79 Y. Ahn, H. Lee, D. Lee and Y. Lee, *ACS Appl. Mater. Interfaces*, 2014, **6**, 18401–18407.
80 M. Singh, S. Rana and A. K. Singh, *Colloid Interface Sci. Commun.*, 2022, **46**, 100563.
81 T. Valayil Varghese, J. Eixenberger, F. Rajabi-Kouchi, M. Lazouskaya, C. Francis, H. Burgoyne, K. Wada, H. Subbaraman and D. Estrada, *ACS Mater. Au*, 2024, **4**, 65–73.
82 M. Alhendi, F. Alshatnawi, E. M. Abbara, R. Sivasubramony, G. Khinda, A. I. Umar, P. Borgesen, M. D. Poliks, D. Shaddock, C.

Hoel, N. Stoffel and T. K. H. Lam, *Addit. Manuf.*, 2022, **54**, 102709.
83 S. Majee, M. C. F. Karlsson, A. Sawatdee, M. Y. Mulla, N. ul H. Alvi, V. Beni and D. Nilsson, *Npj Flex. Electron.*, 2021, **5**, 1–8.
84 P. Yang, J. Li, S. W. Lee and H. J. Fan, *Adv. Sci.*, 2022, **9**, 2103894.
85 J. Zhang, X. L. Li, S. Fan, S. Huang, D. Yan, L. Liu, P. Valdivia y Alvarado and H. Y. Yang, *Mater. Today Energy*, 2020, **16**, 100407.
86 X. Aeby, X. Yan, T. Huber, A. Schneider, G. Siqueira and G. Nyström, *Adv. Mater. Technol.*, 2025, **10**, 2401132.
87 I. Kim, Y. Kim, K. Woo, E.-H. Ryu, K.-Y. Yon, G. Cao and J. Moon, *RSC Adv.*, 2013, **3**, 15169–15177.
88 Z. Niu, F. Cui, Y. Yu, N. Becknell, Y. Sun, G. Khanarian, D. Kim, L. Dou, A. Dehestani, K. Schierle-Arndt and P. Yang, *J. Am. Chem. Soc.*, 2017, **139**, 7348–7354.
89 S. Jeong, K. Woo, D. Kim, S. Lim, J. S. Kim, H. Shin, Y. Xia and J. Moon, *Adv. Funct. Mater.*, 2008, **18**, 679–686.
90 B. K. Park, D. Kim, S. Jeong, J. Moon and J. S. Kim, *Thin Solid Films*, 2007, **515**, 7706–7711.
91 J. Ryu, H.-S. Kim and H. T. Hahn, *J. Electron. Mater.*, 2011, **40**, 42–50.
92 S. Yokoyama, J. Nozaki, K. Motomiya, N. Tsukahara and H. Takahashi, *Colloids Surf. Physicochem. Eng. Asp.*, 2020, **591**, 124567.
93 Y. Gu, A. Wu, J. F. Federici and X. Zhang, *Chem. Eng. J.*, 2017, **313**, 27–36.
94 A. Sheng, S. Khuje, Z. Li, J. Yu and S. Ren, *ACS Appl. Electron. Mater.*, 2022, **4**, 5558–5564.
95 M. T. Rahman, C. Y. Cheng, B. Karagoz, M. Renn, M. Schrandt, A. Gellman and R. Panat, *ACS Appl. Nano Mater.*, 2019, **2**, 3280–3291.
96 A. Sels and V. Subramanian, *ACS Omega*, 2023, **8**, 1929–1936.
97 S. Shukla, K. Domican, K. Karan, S. Bhattacharjee and M. Secanell, *Electrochimica Acta*, 2015, **156**, 289–300.
98 M. Özkan, S. G. Hashmi, J. Halme, A. Karakoç, T. Sarikka, J. Paltakari and P. D. Lund, *Org. Electron.*, 2017, **44**, 159–167.
99 M. Zea, A. Moya, M. Fritsch, E. Ramon, R. Villa and G. Gabriel, *ACS Appl. Mater. Interfaces*, 2019, **11**, 15160–15169.
100 P. V. Arsenov, A. A. Efimov and V. V. Ivanov, *Polymers*, 2021, **13**, 918.
101 T. D. Grant, A. C. Hourd, S. Zolotovskaya, J. B. Lowe, R. J. Rothwell, T. D. A. Jones and A. Abdolvand, *Mater. Des.*, 2022, **214**, 110377.
102 N. McKibben, M. Curtis, O. Maryon, M. Sawyer, M. Lazouskaya, J. Eixenberger, Z. Deng and D. Estrada, *ACS Appl. Electron. Mater.*, 2024, **6**, 748–760.
103 E. B. Secor, N. S. Bell, M. P. Romero, R. R. Tafoya, T. H. Nguyen and T. J. Boyle, *Nanoscale*, 2022, **14**, 12651–12657.
104 Y. Zhang, Y. Wang, Q. Jiang, J. K. El-Demellawi, H. Kim and H. N. Alshareef, *Adv. Mater.*, 2020, **32**, 1908486.
105 X. Li, Z. Huang, C. E. Shuck, G. Liang, Y. Gogotsi and C. Zhi, *Nat. Rev. Chem.*, 2022, **6**, 389–404.
106 Z. Aghayar, M. Malaki and Y. Zhang, *Nanomaterials*, 2022, **12**, 4346.
107 Y. Wu, D. Zhao, J. Zhang, A. Lin, Y. Wang, L. Cao, S. Wang, S. Xiong and F. Gu, *ACS Omega*, 2021, **6**, 33067–33074.
108 S. Siva, G. A. Bodkhe, C. Cong, S. Hyun Kim and M. Kim, *Chem. Eng. J.*, 2024, **479**, 147492.
109 A. Saleh, S. Wustoni, E. Bihar, J. K. El-Demellawi, Y. Zhang, A. Hama, V. Druet, A. Yudhanto, G. Lubineau, H. N. Alshareef and S. Inal, *J. Phys. Mater.*, 2020, **3**, 044004.
110 T. Y. Ko, D. Kim, S. J. Kim, H. Kim, A. S. Nissimagoudar, S.-C. Lee, X. Lin, P. T. Cummings, S. Doo, S. Park, T. Hassan, T. Oh, A. Chae, J. Lee, Y. Gogotsi, I. In and C. M. Koo, *ACS Nano*, 2023, **17**, 1112–1119.
111 E. B. Secor, T. Z. Gao, A. E. Islam, R. Rao, S. G. Wallace, J. Zhu, K. W. Putz, B. Maruyama and M. C. Hersam, *Chem. Mater.*, 2017, **29**, 2332–2340.
112 H.-Y. Jun, S.-J. Kim and C.-H. Choi, *Nanomaterials*, 2021, **11**, 3441.
113 E. S. Agudosi, E. C. Abdullah, A. Numan, N. M. Mubarak, M. Khalid and N. Omar, *Crit. Rev. Solid State Mater. Sci.*, 2020, **45**, 339–377.
114 A. E. Niaraki Asli, J. Guo, P. L. Lai, R. Montazami and N. N. Hashemi, *Biosensors*, 2020, **10**, 6.
115 K. Pan, Y. Fan, T. Leng, J. Li, Z. Xin, J. Zhang, L. Hao, J. Gallop, K. S. Novoselov and Z. Hu, *Nat. Commun.*, 2018, **9**, 5197.
116 F. Chen, D. Varghese, S. T. McDermott, I. George, L. Geng and D. H. Adamson, *Sci. Rep.*, 2020, **10**, 18047.
117 D. S. Kim, J.-M. Jeong, H. J. Park, Y. K. Kim, K. G. Lee and B. G. Choi, *Nano-Micro Lett.*, 2021, **13**, 87.
118 X. Zhou, T. Leng, K. Pan, Y. Liu, Z. Zhang, J. Li, K. S. Novoselov and Z. Hu, *Carbon*, 2024, **218**, 118693.
119 F. Torrisi, T. Hasan, W. Wu, Z. Sun, A. Lombardo, T. S. Kulmala, G.-W. Hsieh, S. Jung, F. Bonaccorso, P. J. Paul, D. Chu and A. C. Ferrari, *ACS Nano*, 2012, **6**, 2992–3006.
120 S. Lv, S. Ye, C. Chen, Y. Zhang, Y. Wu, Y. Wang, R. Tang, M. M. De Souza, X. Liu and X. Zhao, *J. Mater. Chem. C*, 2021, **9**, 13182–13192.
121 E. B. Secor, Dissertation, Northwestern University, 2017.
122 M. Orrill, D. Abele, M. Wagner and S. LeBlanc, *J. Colloid Interface Sci.*, 2020, **566**, 454–462.
123 Y. Gao, W. Shi, W. Wang, Y. Leng and Y. Zhao, *Ind. Eng. Chem. Res.*, 2014, **53**, 16777–16784.
124 H. Shen, L. Zhang, M. Liu and Z. Zhang, *Theranostics*, 2012, **2**, 283–294.
125 Meenakshi, S. K. Shukla, J. Narang, V. Kumar, P. P. Govender, A. Niv, C. M. Hussain, R. Wang, B. Mangla and R. S. Babu, *Chemosensors*, 2020, **8**, 45.
126 M. Ioniţă, G. M. Vlăsceanu, A. A. Watzlawek, S. I. Voicu, J. S. Burns and H. Iovu, *Compos. Part B Eng.*, 2017, **121**, 34–57.
127 A. Krishnakumar, R. K. Mishra, S. Kadian, A. Zareei, U. H. Rivera and R. Rahimi, *Anal. Chim. Acta*, 2022, **1229**, 340332.
128 D. Minta, Z. González, S. Melendi-Espina and G. Gryglewicz, *Prog. Org. Coat.*, 2023, **185**, 107942.
129 N. Graddage, T. Y. Chu, H. Ding, C. Py, A. Dadvand and Y. Tao, *Org. Electron.*, 2016, **29**, 114–119.
130 M. N. Tousignant, V. Tischler, K. Wagner, Z. S. Lin, J. Brusso, R. Izquierdo and B. H. Lessard, *Flex. Print. Electron.*, 2024, **9**, 015012.
131 T. Lehnert, P. Herbeck-Engel, J. Adam, G. Klein, T. Kololuoma and M. Veith, *Adv. Eng. Mater.*, 2010, **12**, 379–384.
132 K. Zou, Z. Zhao, Z. Gui, M. Xu, L. Chen, X. Li and J. Zhang, *Mater. Sci. Eng. B*, 2025, **318**, 118244.
133 Z. Zhu, J. Zhang, Z. Zhou, H. Ning, W. Cai, J. Wei, S. Zhou, R. Yao, X. Lu and J. Peng, *ACS Appl. Mater. Interfaces*, 2019, **11**, 5193–5199.
134 Y. Liang, J. Yong, Y. Yu, A. Nirmalathas, K. Ganesan, R. Evans, B. Nasr and E. Skafidas, *ACS Nano*, 2019, **13**, 13957–13964.
135 L. Gillan, S. Li, J. Lahtinen, C. Chang, A. Alastalo and J. Leppäniemi, *Adv. Mater. Interfaces*, 2021, **8**, 2100728.
136 E. Carlos, R. Branquinho, R. Martins and E. Fortunato, *Solid-State Electron.*, 2021, **183**, 108044.

137 J. Hwang, K. Lee, Y. Jeong, Y. U. Lee, C. Pearson, M. C. Petty and H. Kim, *Adv. Mater. Interfaces*, 2014, **1**, 1400206.
138 S. K. Sarkar, D. Maji, J. A. Khan, S. Kurup and D. Gupta, *ACS Appl. Electron. Mater.*, 2022, **4**, 2442–2454.
139 E. Carlos, R. Martins, E. Fortunato and R. Branquinho, *Chem. – Eur. J.*, 2020, **26**, 9099–9125.
140 Y. W. Oh, H. Kim, L. M. Do, K. H. Baek, I. S. Kang, G. W. Lee and C. M. Kang, *RSC Adv.*, 2024, **14**, 37438–37444.
141 D. Wickramaratne, L. Weston and C. G. Van De Walle, *J. Phys. Chem. C*, 2018, **122**, 25524–25529.
142 G. U. Siddiqui, M. M. Rehman, Y. J. Yang and K. H. Choi, *J. Mater. Chem. C*, 2017, **5**, 862–871.
143 P. Zhang, F. Dang, X. Zhang, C. Nan and B. Li, *Small*, 2024, **20**, 2404581.
144 P. Zhang, Y. Fu, X. Zhang, X. Zhang, B.-W. Li and C.-W. Nan, *Sci. Bull.*, 2022, **67**, 2541–2549.
145 X. Wu, F. Fei, Z. Chen, W. Su and Z. Cui, *Compos. Sci. Technol.*, 2014, **94**, 117–122.
146 H. Abdolmaleki and S. Agarwala, *Polymers*, 2020, **12**, 2430.
147 M. Mikolajek, T. Reinheimer, N. Bohn, C. Kohler, M. J. Hoffmann and J. R. Binder, *Sci. Rep.*, 2019, **9**, 13324.
148 T. Carey, S. Cacovich, G. Divitini, J. Ren, A. Mansouri, J. M. Kim, C. Wang, C. Ducati, R. Sordan and F. Torrisi, *Nat. Commun.*, 2017, **8**, 1202.
149 R. Buchheit, B. Kuttich, L. González-García and T. Kraus, *Adv. Mater.*, 2021, **33**, 2103087.
150 Y. Li, L. Jing, X. Xiong, R. Tao, Z. Fan, X. Lu, G. Zhou, Z. Fang, H. Ning and J. Liu, *Surf. Interfaces*, 2024, **44**, 103666.
151 A. Singh, S. K. Gupta and A. Garg, *Sci. Rep.*, 2017, **7**, 1775.
152 H. Hu, J. Zhu, M. Chen, T. Guo and F. Li, *Appl. Surf. Sci.*, 2018, **441**, 295–302.
153 M. Wei, M. Robin, L. Portilla, Y. Ren, S. Shao, L. Bai, Y. Cao, V. Pecunia, Z. Cui and J. Zhao, *Carbon*, 2020, **163**, 145–153.
154 A. A. Gupta, S. Arunachalam, S. G. Cloutier and R. Izquierdo, *ACS Photonics*, 2018, **5**, 3923–3929.
155 H. Okimoto, T. Takenobu, K. Yanagi, Y. Miyata, H. Shimotani, H. Kataura and Y. Iwasa, *Adv. Mater.*, 2010, **22**, 3981–3986.
156 S. Lu and A. D. Franklin, *Nanoscale*, 2020, **12**, 23371–23390.
157 M. Ha, Y. Xia, A. A. Green, W. Zhang, M. J. Renn, C. H. Kim, M. C. Hersam and C. D. Frisbie, *ACS Nano*, 2010, **4**, 4388–4395.
158 C. Cao, J. B. Andrews and A. D. Franklin, *Adv. Electron. Mater.*, 2017, **3**, 1700057.
159 P. Guo, M. Li, S. Shao, Y. Fang, Z. Chen, H. Guo and J. Zhao, *Carbon*, 2023, **215**, 118453.
160 S. Lu, B. N. Smith, H. Meikle, M. J. Therien and A. D. Franklin, *Nano Lett.*, 2023, **23**, 2100–2106.
161 J. Park, H. W. Choi and B. Kim, *ACS Appl. Electron. Mater.*, 2023, **5**, 552–558.
162 W. Xu, Z. Liu, J. Zhao, W. Xu, W. Gu, X. Zhang, L. Qian and Z. Cui, *Nanoscale*, 2014, **6**, 14891–14897.
163 M. Moreira, E. Carlos, C. Dias, J. Deuermeier, M. Pereira, P. Barquinha, R. Branquinho, R. Martins and E. Fortunato, *Nanomaterials*, 2019, **9**, 1273.
164 E. B. Secor, J. Smith, T. J. Marks and M. C. Hersam, *ACS Appl. Mater. Interfaces*, 2016, **8**, 17428–17434.
165 H. Huang, H. Hu, J. Zhu and T. Guo, *J. Electron. Mater.*, 2017, **46**, 4497–4502.
166 S. Choi, K.-T. Kim, S. K. Park and Y.-H. Kim, *Materials*, 2019, **12**, 852.
167 L. Magnarin, B. Breitung and J. Aghassi-Hagmann, *Adv. Electron. Mater.*, 2025, **11**, 2400478.
168 M. Franco, A. Kiazadeh, J. Deuermeier, S. Lanceros-Méndez, R. Martins and E. Carlos, *Sci. Rep.*, 2024, **14**, 7469.
169 Y. K. Shen, Z. Liu, X. L. Wang, W. K. Ma, Z. H. Chen, T. P. Chen and H. Y. Zhang, *Solid-State Electron.*, 2017, **138**, 108–112.
170 M. Franco, A. Kiazadeh, J. Deuermeier, S. Lanceros-Méndez, R. Martins and E. Carlos, *Sci. Rep.*, 2024, **14**, 7469.
171 T. K. Chaudhuri, M. H. Patel, D. Tiwari and P. R. Ghediya, *J. Alloys Compd.*, 2018, **747**, 31–37.
172 A. Glushkova, P. Andričević, R. Smajda, B. Náfrádi, M. Kollár, V. Djokić, A. Arakcheeva, L. Forró, R. Pugin and E. Horváth, *ACS Nano*, 2021, **15**, 4077–4084.
173 Y. Liu, Q. Zhang, A. Huang, K. Zhang, S. Wan, H. Chen, Y. Fu, W. Zuo, Y. Wang, X. Cao, L. Wang, U. Lemmer and W. Jiang, *Nat. Commun.*, 2024, **15**, 2141.
174 C. Dun, W. Kuang, N. Kempf, M. Saeidi-Javash, D. J. Singh and Y. Zhang, *Adv. Sci.*, 2019, **6**, 1901788.
175 M. Saeidi-Javash, W. Kuang, C. Dun and Y. Zhang, *Adv. Funct. Mater.*, 2019, **29**, 3–8.
176 G. Hu, L. Yang, Z. Yang, Y. Wang, X. Jin, J. Dai, Q. Wu, S. Liu, X. Zhu, X. Wang, T.-C. Wu, R. C. T. Howe, T. Albrow-Owen, L. W. T. Ng, Q. Yang, L. G. Occhipinti, R. I. Woodward, E. J. R. Kelleher, Z. Sun, X. Huang, M. Zhang, C. D. Bain and T. Hasan, *Sci. Adv.*, 2020, **6**, eaba5029.
177 S. Pinilla, J. Coelho, K. Li, J. Liu and V. Nicolosi, *Nat. Rev. Mater.*, 2022, **7**, 717–735.
178 S. Conti, G. Calabrese, K. Parvez, L. Pimpolari, F. Pieri, G. Iannaccone, C. Casiraghi and G. Fiori, *Nat. Rev. Mater.*, 2023, **8**, 651–667.
179 D. Jang, D. Kim and J. Moon, *Langmuir*, 2009, **25**, 2629–2635.
180 I. A. Volkov, N. P. Simonenko, A. A. Efimov, T. L. Simonenko, I. S. Vlasov, V. I. Borisov, P. V. Arsenov, Y. Y. Lebedinskii, A. M. Markeev, A. A. Lizunova, A. S. Mokrushin, E. P. Simonenko, V. A. Buslov, A. E. Varfolomeev, Z. Liu, A. A. Vasiliev and V. V. Ivanov, *Appl. Sci.*, 2021, **11**, 526.
181 Y. Piro, C. Areias, A. Luce, M. Michael, P. Biswas, O. Ranasingha, J. F. Reuther, S. Trulli and A. Akyurtlu, *ACS Appl. Mater. Interfaces*, 2023, **15**, 35449–35458.
182 A. Roshanghias, M. Krivec and M. Baumgart, *Flex. Print. Electron.*, 2017, **2**, 045002.
183 N. Turan, M. Saeidi-Javash, J. Chen, M. Zeng, Y. Zhang and D. B. Go, *ACS Appl. Mater. Interfaces*, 2021, **13**, 47244–47251.
184 A. Albrecht, A. Rivadeneyra, A. Abdellah, P. Lugli and J. F. Salmerón, *J. Mater. Chem. C*, 2016, **4**, 3546–3554.
185 L. Zhou, X. Chen, W. Su, Z. Cui and W.-Y. Lai, *Adv. Mater. Interfaces*, 2022, **9**, 2102548.
186 K. S. Bhat, U. T. Nakate, J. Y. Yoo, Y. Wang, T. Mahmoudi and Y. B. Hahn, *Chem. Eng. J.*, 2019, **373**, 355–364.
187 I. J. Fernandes, A. F. Aroche, A. Schuck, P. Lamberty, C. R. Peter, W. Hasenkamp and T. L. A. C. Rocha, *Sci. Rep.*, 2020, **10**, 8878.
188 W. Yang, F. Mathies, E. L. Unger, F. Hermerschmidt and E. J. W. List-Kratochvil, *J. Mater. Chem. C*, 2020, **8**, 16443–16451.
189 M. S. Saleh, S. M. Ritchie, M. A. Nicholas, H. L. Gordon, C. Hu, S. Jahan, B. Yuan, R. Bezbaruah, J. W. Reddy, Z. Ahmed, M. Chamanzar, E. A. Yttri and R. P. Panat, *Sci. Adv.*, **8**, eabj4853.
190 S. J. DiGregorio, S. Raikar and O. J. Hildreth, *ACS Appl. Electron. Mater.*, 2024, **6**, 203–213.
191 T. S.-W. Leung, E. Ramon and C. Martínez-Domingo, *Adv. Eng. Mater.*, 2023, **25**, 2200834.
192 S. H. Ko, H. Pan, C. P. Grigoropoulos, C. K. Luscombe, J. M. J. Fréchet and D. Poulikakos, *Nanotechnology*, 2007, **18**, 345202.

193 S. Ma, V. Bromberg, L. Liu, F. D. Egitto, P. R. Chiarot and T. J. Singler, *Appl. Surf. Sci.*, 2014, **293**, 207–215.
194 A. Sharif, N. Farid and G. M. O'Connor, *Results Eng.*, 2022, **16**, 100731.
195 H. W. Tan, N. Saengchairat, G. L. Goh, J. An, C. K. Chua and T. Tran, *Adv. Mater. Technol.*, 2020, **5**, 1900897.
196 Y. Sui, L. Tsui, A. J. Thibodeaux and J. M. Lavin, *Adv. Mater. Technol.*, 2023, **8**, 2202053.
197 D. Reenaers, W. Marchal, I. Biesmans, P. Nivelle, J. D'Haen and W. Deferme, *Nanomaterials*, 2020, **10**, 892.
198 Z. Chen, U. Gengenbach, L. Koker, L. Huang, T. P. Mach, K. Reichert, R. Thelen and M. Ungerer, *Small*, 2024, **20**, 2306865.
199 V. Correia, K. Y. Mitra, H. Castro, J. G. Rocha, E. Sowade, R. R. Baumann and S. Lanceros-Mendez, *J. Manuf. Process.*, 2018, **31**, 364–371.
200 E. Enakerakpo, M. Alhendi, G. S. Khinda, B. Garakani, K. U. Sandekelum Somarathna, M. Poliks, S. Gonya and V. Basava, in *2021 IEEE 71st Electronic Components and Technology Conference (ECTC)*, IEEE, San Diego, CA, USA, 2021, pp. 1138–1143.
201 H. F. Castro, V. Correia, E. Sowade, K. Y. Mitra, J. G. Rocha, R. R. Baumann and S. Lanceros-Méndez, *Org. Electron.*, 2016, **38**, 205–212.
202 Y. Gu, D. Park, D. Bowen, S. Das and D. R. Hines, *Adv. Mater. Technol.*, 2019, **4**, 1800312.
203 X. Konstantinou, X. Lan, K. Nguyen, A. Escorcia, R. Sandhu, J. Tice, W. Spain, J. D. Albrecht and J. Papapolymerou, *IEEE Microw. Wirel. Technol. Lett.*, 2023, **33**, 511–514.
204 M. T. Craton, X. Konstantinou, J. D. Albrecht, P. Chahal and J. Papapolymerou, *IEEE Trans. Microw. Theory Tech.*, 2021, **69**, 4191–4198.
205 E. S. Rosker, M. T. Barako, E. Nguyen, V. Radisic, M. S. Goorsky and J. Tice, *Flex. Print. Electron.*, 2022, **7**, 035006.
206 S. Y. Jun, A. Elibiary, B. Sanz-Izquierdo, L. Winchester, D. Bird and A. McCleland, *IEEE Trans. Compon. Packag. Manuf. Technol.*, 2018, **8**, 2227–2235.
207 K. Hu, Y. Zhou, S. K. Sitaraman and M. M. Tentzeris, *Sci. Rep.*, 2023, **13**, 12515.
208 P. Li, J. Fleischer, E. Quinn and D. Park, *J. Manuf. Mater. Process.*, 2024, **8**, 39.
209 N. Langford and S. Shina, in *2019 Pan Pacific Microelectronics Symposium (Pan Pacific)*, IEEE, Kauai, HI, USA, 2019, pp. 1–16.
210 E. Gupta, C. Bonner, N. Lazarus, M. S. Mirotznik and K. J. Nicholson, *IEEE Antennas Wirel. Propag. Lett.*, 2023, **22**, 2629–2633.
211 C. Areias and A. Akyurtlu, *Adv. Eng. Mater.*, 2025, 2402715.
212 E. S. Rosker, M. T. Barako, E. Nguyen, D. DiMarzio, K. Kisslinger, D.-W. Duan, R. Sandhu, M. S. Goorsky and J. Tice, *ACS Appl. Mater. Interfaces*, 2020, acsami.0c06959.
213 Y. Khan, M. Garg, Q. Gui, M. Schadt, A. Gaikwad, D. Han, N. A. D. Yamamoto, P. Hart, R. Welte, W. Wilson, S. Czarnecki, M. Poliks, Z. Jin, K. Ghose, F. Egitto, J. Turner and A. C. Arias, *Adv. Funct. Mater.*, 2016, **26**, 8764–8775.
214 C. Oakley, J. D. Albrecht, J. Papapolymerou and P. Chahal, *IEEE Trans. Compon. Packag. Manuf. Technol.*, 2019, **9**, 2305–2313.
215 J. Krzeminski, A. Kanthamneni, D. Wagner, M. Detert, B. Schmidt and M. Jakubowska, *IEEE Trans. Nanotechnol.*, 2018, **17**, 979–984.
216 S. Vella, C. S. Smithson, K. Halfyard, E. Shen and M. Chrétien, *Flex. Print. Electron.*, 2019, **4**, 045005.
217 L. Rauter, J. Zikulnig, T. Sinani, H. Zangl and L.-M. Faller, *Electron. Mater.*, 2020, **1**, 2–16.
218 K. Werum, E. Mueller, J. Keck, J. Jaeger, T. Horter, K. Glaeser, S. Buschkamp, M. Barth, W. Eberhardt and A. Zimmermann, *J. Manuf. Mater. Process.*, 2022, **6**, 119.
219 D. R. Hines, Y. Gu, A. A. Martin, P. Li, J. Fleischer, A. Clough-Paez, G. Stackhouse, A. Dasgupta and S. Das, *Addit. Manuf.*, 2021, **47**, 102325.
220 A. Smirnov, A. Polushkin, A. Falchevskaya, M. Mikhailova, H. Shamkhi, L. Zelenkov, T. Pogosian, M. Morozov, S. Makarov and A. Vinogradov, *Adv. Opt. Mater.*, 2023, **11**, 2300385.
221 T. Reitberger, J. Hoerber, R. Schramm, S. Sennefelder and J. Franke, in *2015 38th International Spring Seminar on Electronics Technology (ISSE)*, IEEE, Eger, Hungary, 2015, pp. 5–10.
222 P. Bollgruen, T. Wolfer, U. Gleissner, D. Mager, C. Megnin, L. Overmeyer, T. Hanemann and J. G. Korvink, *Flex. Print. Electron.*, 2017, **2**, 045003.
223 J. Dominiczak, J. Krzemiński, J. Wojcieszek, D. Baraniecki, F. Budny, I. Wojciechowska, P. Walter, A. Pepłowski, Ł. Górski and M. Jakubowska, *Sens. Bio-Sens. Res.*, 2024, **43**, 100636.
224 Z. Lin, T. Le, X. Song, Y. Yao, Z. Li, K. Moon, M. M. Tentzeris and C. Wong, *J. Electron. Packag.*, 2013, **135**, 011001.
225 M.-A. Nalepa, D. Panáček, I. Dědek, P. Jakubec, V. Kupka, V. Hrubý, M. Petr and M. Otyepka, *Biosens. Bioelectron.*, 2024, **256**, 116277.
226 M. Tursunniyaz, A. Meredith and J. Andrews, *Sens. Actuators Phys.*, 2023, **364**, 114777.
227 P. Karipoth, J. H. Chandler, J. Lee, S. Taccola, J. Macdonald, P. Valdastri and R. A. Harris, *Adv. Eng. Mater.*, 2024, **26**, 2301275.
228 Q. Wang, G. Zhang, H. Zhang, Y. Duan, Z. Yin and Y. Huang, *Adv. Funct. Mater.*, 2021, **31**, 2100857.
229 M. M. R. Momota, B. I. Morshed, T. Ferdous and T. Fujiwara, *IEEE Sens. J.*, 2023, **23**, 7917–7928.
230 B. Clifford, D. Beynon, C. Phillips and D. Deganello, *Sens. Actuators B Chem.*, 2018, **255**, 1031–1038.
231 Y. Hou, M. Gao, J. Gao, L. Zhao, E. H. T. Teo, D. Wang, H. J. Qi and K. Zhou, *Adv. Sci.*, 2023, **10**, 2304132.
232 H. Zhang and S. K. Moon, *ACS Appl. Mater. Interfaces*, 2021, **13**, 53323–53345.
233 F. Wang, M. Elbadawi, S. L. Tsilova, S. Gaisford, A. W. Basit and M. Parhizkar, *Mater. Sci. Eng. C*, 2022, **132**, 112553.
234 J. R. Deneault, J. Chang, J. Myung, D. Hooper, A. Armstrong, M. Pitt and B. Maruyama, *MRS Bull.*, 2021, **46**, 566–575.
235 M. Ogunsanya, J. Isichei, S. K. Parupelli, S. Desai and Y. Cai, *Procedia Manuf.*, 2021, **53**, 427–434.
236 S. Kim, M. Cho and S. Jung, *Sci. Rep.*, 2022, **12**, 4841.
237 F. P. Brishty, R. Urner and G. Grau, *Flex. Print. Electron.*, 2022, **7**, 15009.
238 M. Polomoshnov, K.-M. Reichert, L. Rettenberger, M. Ungerer, G. Hernandez-Sosa, U. Gengenbach and M. Reischl, *J. Intell. Manuf.*, 2025, **36**, 2709–2726.
239 H. Zhang, S. K. Moon and T. H. Ngo, *ACS Appl. Mater. Interfaces*, 2019, **11**, 17994–18003.
240 R. (Ross) Salary, J. P. Lombardi, D. L. Weerawarne, M. S. Tootooni, P. K. Rao and M. D. Poliks, *J. Manuf. Sci. Eng.*, 2020, **142**, 081007.
241 Y. Liu, S. Yin, Z. Liu and H. Zhang, *Flex. Print. Electron.*, 2023, **8**, 25017.
242 Y. Du, M. Jiang and Y. Zhang, *Adv. Mater. Technol.*, 2024, **9**, 2301286.

243 M. Abbasi Shirsavar, M. Taghavimehr, L. J. Ouedraogo, M. Javaheripi, N. N. Hashemi, F. Koushanfar and R. Montazami, *Biosens. Bioelectron.*, 2022, **212**, 114418.

244 T. Dong, J.-X. Wang, Y. Wang, G.-H. Tang, Y. Cheng and W.-C. Yan, *Chem. Eng. Sci.*, 2023, **268**, 118398.

245 S. K. Singh, N. Rai and A. Subramanian, *Adv. Eng. Mater.*, 2023, **25**, 2300740.

246 L. Jiang, R. Wolf, K. Alharbi and H. Qin, *J. Manuf. Sci. Eng.*, 2024, **146**, 110901.

247 J. Chen, Y. Yuan, Q. Wang, H. Wang and R. C. Advincula, *Nanomaterials*, 2025, **15**, 843.

248 J. Jiang, Y. Xiong, Z. Zhang and D. W. Rosen, *J. Intell. Manuf.*, 2022, **33**, 1073–1086.

249 H. Yun, H.-C. Liao, J. Borenstein, B. Davaji, P. C. Doerschuk and A. Lal, in *2025 36th Annual SEMI Advanced Semiconductor Manufacturing Conference (ASMC)*, IEEE, Albany, NY, USA, 2025, pp. 1–6.

250 X. Zhao, Y. Sun, Y. Li, N. Jia and J. Xu, *Meas. Sci. Technol.*, 2025, **36**, 012003.

251 R. (Ross) Salary, J. P. Lombardi, D. L. Weerawarne, P. K. Rao and M. D. Poliks, in *Volume 2: Advanced Manufacturing*, American Society of Mechanical Engineers, Pittsburgh, Pennsylvania, USA, 2018, p. V002T02A057.

252 R. (Ross) Salary, J. P. Lombardi, D. L. Weerawarne, P. Rao and M. D. Poliks, *J. Micro Nano-Manuf.*, 2021, **9**, 010903.

253 G. Chen, Y. Gu, H. Tsang, D. R. Hines and S. Das, *Adv. Eng. Mater.*, 2018, **20**, 1701084.

254 S. Ramesh, Z. Xu, I. V. Rivero and D. R. Cormier, *J. Manuf. Process.*, 2023, **95**, 312–329.

255 L. Jiang, L. Yu, P. Premaratne, Z. Zhang and H. Qin, *J. Manuf. Process.*, 2021, **66**, 125–132.

256 T. J. Ober, D. Foresti and J. A. Lewis, *Proc. Natl. Acad. Sci.*, 2015, **112**, 12293–12298.

257 N. C. Brown, D. C. Ames and J. Mueller, *Nat. Rev. Mater.*, DOI:10.1038/s41578-025-00809-y.

258 M. Sukeshini A., F. Meisenkothen, P. Gardner and T. L. Reitz, *J. Power Sources*, 2013, **224**, 295–303.

259 K. Wang, Y.-H. Chang, C. Zhang and B. Wang, *Carbon*, 2016, **98**, 397–403.

260 M. T. Craton, J. D. Albrecht, P. Chahal and J. Papapolymerou, *IEEE Trans. Compon. Packag. Manuf. Technol.*, 2021, **11**, 865–871.

261 M. T. Craton, J. D. Albrecht, P. Chahal and J. Papapolymerou, *IEEE Trans. Microw. Theory Tech.*, 2020, **68**, 1646–1659.

262 M. Zeng, Y. Du, Q. Jiang, N. Kempf, C. Wei, M. V. Bimrose, A. N. M. Tanvir, H. Xu, J. Chen, D. J. Kirsch, J. Martin, B. C. Wyatt, T. Hayashi, M. Saeidi-Javash, H. Sakaue, B. Anasori, L. Jin, M. D. McMurtrey and Y. Zhang, *Nature*, 2023, **617**, 292–298.

263 Q. Jiang, S. Atampugre, Y. Du, L. Yang, J. L. Schaefer and Y. Zhang, *ACS Mater. Lett.*, 2024, **6**, 2205–2212.

264 L. Gamba, J. A. Lajoie, T. R. Sippel and E. B. Secor, *Adv. Funct. Mater.*, 2023, **33**, 2304060.

265 L. Gamba, M. E. A. Razzaq, S. Diaz-Arauzo, M. C. Hersam, X. Bai and E. B. Secor, *ACS Appl. Mater. Interfaces*, 2023, **15**, 57525–57532.

266 K. Song, J. Zhou, C. Wei, A. Ponnuchamy, M. O. Bappy, Y. Liao, Q. Jiang, Y. Du, C. J. Evans, B. C. Wyatt, T. O' Sullivan, R. K. Roeder, B. Anasori, A. J. Hoffman, L. Jin, X. Duan and Y. Zhang, *Adv. Mater.*, DOI:10.1002/adma.202414203.

267 M. S. Saleh, S. M. Ritchie, M. A. Nicholas, H. L. Gordon, C. Hu, S. Jahan, B. Yuan, R. Bezbaruah, J. W. Reddy, Z. Ahmed, M. Chamanzar, E. A. Yttri and R. P. Panat, *Sci. Adv.*, 2022, **8**, 1–15.

268 G. L. Goh, V. Dikshit, R. Koneru, Z. K. Peh, W. Lu, G. D. Goh and W. Y. Yeong, *Int. J. Adv. Manuf. Technol.*, 2022, **120**, 2573–2586.

269 J. Jiang, B. Bao, M. Li, J. Sun, C. Zhang, Y. Li, F. Li, X. Yao and Y. Song, *Adv. Mater.*, 2016, **28**, 1420–1426.

270 Y. Li, R. Wang, X. Zhu, J. Yang, L. Zhou, S. Shang, P. Sun, W. Ge, Q. Xu and H. Lan, *Adv. Eng. Mater.*, 2023, **25**, 2200785.

271 T. Tilford, S. Stoyanov, J. Braun, J. C. Janhsen, M. Burgard, R. Birch and C. Bailey, *Microelectron. Reliab.*, 2018, **85**, 109–117.

272 T. Tilford, S. Stoyanov, J. Braun, J. C. Janhsen, M. K. Patel and C. Bailey, *IEEE Trans. Compon. Packag. Manuf. Technol.*, 2021, **11**, 351–362.

273 G. M. Williams and J. Paul Harmon, *Opt. Contin.*, 2023, **2**, 456.

274 H. Yi, X. Guo, F. Chang, H. Cao, J. An and C. K. Chua, *Int. J. Extreme Manuf.*, 2025, **7**, 032002.

275 C. Fisher, L. N. Skolrood, K. Li, P. C. Joshi and T. Aytug, *Adv. Mater. Technol.*, 2023, **8**, 2300030.

276 M. Davies, M. J. Hobbs, J. Nohl, B. Davies, C. Rodenburg and J. R. Willmott, *Sci. Rep.*, DOI:10.1038/s41598-022-23292-9.

277 D. J. Richmond, E. Enakerakpo, M. Alhendi, P. McClure and M. D. Poliks, in *2022 IEEE 72nd Electronic Components and Technology Conference (ECTC)*, IEEE, San Diego, CA, USA, 2022, pp. 2298–2304.

278 J. Q. Feng, *Aerosol Sci. Technol.*, 2019, **53**, 45–52.

279 J. D. Rurup and E. B. Secor, *J. Manuf. Process.*, 2024, **120**, 1231–1240.

280 H. A. Hobbie, J. L. Doherty, B. N. Smith, P. Maccarini and A. D. Franklin, *Npj Flex. Electron.*, 2024, **8**, 54.

281 E. Gupta, C. Bonner, N. Lazarus, M. S. Mirotznik and K. J. Nicholson, *IEEE Antennas Wirel. Propag. Lett.*, 2023, **22**, 2629–2633.

282 Y. Gu, D. Park, S. Gonya, J. Jendrisak, S. Das and D. R. Hines, *Addit. Manuf.*, 2019, **30**, 100843.

283 M. S. Saleh, J. Li, J. Park and R. Panat, *Addit. Manuf.*, 2018, **23**, 70–78.

284 L. Gamba, S. Diaz-Arauzo, M. C. Hersam and E. B. Secor, *ACS Appl. Nano Mater.*, 2023, **6**, 21133–21140.

285 C. Areias, Y. Piro, O. Ranasingha and A. Akyurtlu, *Flex. Print. Electron.*, 2023, **8**, 15009.

286 S. Ma, A. S. Dahiya and R. Dahiya, *Adv. Mater.*, 2023, **35**, 2210711.

287 R. Kaufhold, S. Khan, J. Kosel and J. Aghassi-Hagmann, in *2024 IEEE International Conference on Flexible and Printable Sensors and Systems (FLEPS)*, 2024, pp. 1–4.

View Article Online
DOI: 10.1039/D5NR02110C

Data availability

No primary research results, software or code have been included and no new data were generated or analysed as part of this review.